Available online http://amq.aiqua.it
ISSN (print): 2279-7327, ISSN (online): 2279-7335

Alpine and Mediterranean Quaternary, 33 (1), 2020, 5-30 https://doi.org/10.26382/AMQ.2020.01

LATEST PLEISTOCENE TO HOLOCENE ENVIRONMENTAL CHANGES IN THE NORTHERN TYRRHENIAN AREA (CENTRAL MEDITERRANEAN). A CASE STUDY FROM SOUTHERN ELBA ISLAND.

Maurizio D'Orefice [1], Roberto Graciotti [1], Adele Bertini [2, 3], Mariaelena Fedi [4], Luca Maria Foresi [5, 6], Marianna Ricci [2], Francesco Toti [2]

[1] ISPRA - Dipartimento per il Servizio Geologico d'Italia, Roma, Italy.
[2] Dipartimento di Scienze della Terra, Università degli Studi di Firenze, Italy.
[3] Istituto di Geoscienze e Georisorse, CNR, Firenze, Italy.
[4] Istituto Nazionale di Fisica Nucleare, Sesto Fiorentino, Firenze, Italy.
[5] Dipartimento di Scienze fisiche, della Terra e dell'Ambiente, Università degli Studi di Siena, Italy.
[6] Istituto di Geoscienze e Georisorse, CNR, Pisa, Italy.

Corresponding authors: A. Bertini <adele.bertini@unifi.it>

ABSTRACT: Geological and geomorphological studies, within the framework of the Geomorphological Sheet "Isola d'Elba" (1:50,000, ISPRA-Servizio Geologico d'Italia) have been implemented by sedimentological, geochronological and biostratigraphical (foraminifers, malacofauna, and palynology) analyses on sedimentary cores retrieved during four continuous mechanical drillings near the Marina di Campo village. Drill cores (S1-S4), up to 23-25 m deep, in sedimentary deposits referable to the last glacio-eustatic cycle allowed the reconstruction of the paleoenvironmental history of the southern sector of the Elba Island, since the Last Glacial Maximum (LGM).
A significant fall in sea level (Lowstand Systems Tract - LST) determines the complete emergence and incision of the Tuscan continental shelf, including the sector in front of Marina di Campo, during the LGM. Thick fluvial sediments, mainly consisting of gravel, sand and silt alternations filled the river incisions. During the subsequent transgressive phase (Transgressive Systems Tract - TST), there was a progressive reduction of fluvial sedimentation and coastline retreat. Starting from about 7,000 cal. yr BP a shallow marine environment extended in the eastern sector of the Marina di Campo plain (S2 at about -10.60 m a.s.l.). Meanwhile, in the innermost portion of the plain dark gray organic clays and silts accumulated in brackish lagoons (S3). In both sector, continental deposits that interrupt marine and lagoon sedimentation, attest a brief regressive episode between ~6,600 and 5,800 cal. yr BP. Immediately after the regressive episode, the sedimentation of sand, sandy silt and biocalcarenites occurs in a relatively deeper sea (S2, between -8.41 and -3.91 m a.s.l.). In the innermost areas, however, organic clays and silts continue to accumulate in lagoons, whereas in upper areas fluvial sedimentation dominates. With the start of the sea level highstand phase (Highstand Systems Tract - HST), around 6,000 cal. yr BP, the ongoing progradation of the barrier-lagoon system determines a regression of the coastline and the eastward extension of brackish lagoons. With the definitive closure of the communication with the open sea, between ca1,500 and 1,300-1,200 cal. yr BP, the Marina di Campo lagoons were progressively transformed into freshwater coastal ponds. In the areas surrounding the ancient coastal ponds, river sedimentation persisted until today as attested by the current floodplain.

Keywords: coastal wetlands, geomorphological survey, stratigraphic cores, ^{14}C dating, micropaleontology, palynology, Holocene, Italy.

1. INTRODUCTION

Coastal plains, especially the Mediterranean ones, include a variety of sedimentary archives which allow documenting the main Quaternary environmental and climatic changes by the use of several geo-chemical and biotic proxies. Many works have been carried out in the coastal plains of Corsica (e.g. Currás et al., 2017; Forzoni et al., 2015), Sardinia (e.g. Melis et al., 2017, 2018; Pascucci et al., 2018) and Italian mainland (Aguzzi et al., 2005; 2007; Amorosi et al., 2008; 2009; 2012; 2013; Bini et al., 2010; 2018). These areas have been the field of investigation for geomorphologists, Quaternary geologists and archeologists that aimed to reconstruct both fluvial and coastal environments. Such multiproxy studies document the prevalent effects of the glacio-eustatic oscillations of the sea level induced by climatic changes, often expressed by an alternation of erosive and depositional phases (e.g. Zaitlin et al., 1994; Blum & Törnqvist, 2000). In this context, systems tracts (lowstand, transgressive and highstand systems tracts) of the high-frequency sequences exhibit a high probability of conservation (Posamentier et al., 1988; Milli et al., 2016 and reference therein). Within the different systems tracts, important changes are frequent in both the channel and stacking patterns of river deposits.

In the last millennia, the stratigraphic architecture of the coastal depositional sequences has been greatly

modified also by anthropic activity (e.g. Brückner et al., 2005; Bellotti et al., 2016; Currás et al., 2017; Di Rita et al., 2018 and references therein; Melis et al., 2018; Pascucci et al., 2018; Sadori, 2018). The assessment of both the human impact and the possible future effects of the global climate change is indispensable for the preservation of coastal areas and ecosystems, which represent important sites of biodiversity, biological productivity, and ecosystem services (e.g. to remove and manage sediments, nutrients, and contaminants from inflowing rivers).

In this context the researches on late Quaternary sedimentary successions of the Elba Island (EI) provide an opportunity to produce new evidence and datasets for a key area of the Mediterranean region. EI is situated in the Northern Tyrrhenian Sea between the Corsica Island to the west and the Italian mainland to the east. It is the largest island of the Tuscan Archipelago (Mediterranean Sea) and the third largest island of the Italian Peninsula with a surface area of 224 km^2. Geological literature on EI principally concerns the well exposed pre-Quaternary deposits (Principi et al., 2015a, b and references therein). Indeed, a few works have focused on the EI Late Pleistocene to Holocene coastal deposits. The more recent field surveys on the main coastal plains of the EI (Geomorphological Sheet "Isola d'Elba" at 1:50,000 scale; ISPRA-Servizio Geologico d'Italia, 2018; D'Orefice & Graciotti, 2018) provided a unique opportunity to document the late Quaternary sedimentary successions by the recovering of several continuous cores in its northern-central and southern-central sectors (D'Orefice et al., 2011) (Fig. 1a, b). In our investigation, field data were significantly integrated by sedimentological, geochronological and biostratigraphical (invertebrate microfossils and palynomorphs) studies in order to reconstruct, for the first time, the main late Quaternary paleoenvironmental changes, in the Elba area, and to correlate them to those acting at regional and global scales.

2. GEOLOGICAL AND GEOMORPHOLOGICAL SETTING

EI (Fig. 1a) represents the westernmost part of the North-Apennine orogenic belt. EI formed by a complex stack of tectonic nappes (Bortolotti et al., 2015; Principi et al., 2015a, b), which sediments refer to Paleozoic (Variscan orogenesis) to Oligocene formations, belonging to both Ligurian and Tuscan domains (Bortolotti et al., 2015; Principi et al., 2015a, b). Such deposits underwent polyphasic compressive deformations from Late Cretaceous to Middle Miocene (Bortolotti et al., 2015; Principi et al., 2015a, b). The post-orogenic extensive phase characterized by low- and high-angle faults developed during an intense magmatic activity. The latter drove the rise of the Monte Capanne monzogranitic pluton in the western part of the EI (~6.9 Ma; Dini et al., 2002), and later the less extensive Porto Azzurro pluton in the Eastern EI (~5.9 Ma; Saupé et al., 1982; Maineri et al., 2003). The location of the intrusive masses promoted the thermo-metamorphism of the enclosing rocks, the topographic uplift of the area and the very last horizontal displacements within the tectonic pile. The predominantly eastward movements caused the anomalous overlap of the previously embricated tectonic units (Bortolotti et al., 2015; Principi et al., 2015a, b). During the latest Miocene - early Pliocene tectonic events high-angle N-S trending normal faults activated especially in the eastern part of the island (Bortolotti et al., 2015; Principi et al., 2015a, b).

The Quaternary sedimentary history of EI was strictly controlled by the glacio-eustatic sea level changes, induced by climatic cyclicities, especially during the last glacial-interglacial cycle when a global sea level drop is recorded (e.g. Waelbroek et al., 2002; Siddal et al., 2003; Lambeck et al., 2011).

During the Last Interglacial highstand in correspondence of the Marine Isotope Stage (MIS) 5.5 (at ~125 kyr BP) the sea level rises of 7 ±2 m a.s.l., in the Italian coast (Ferranti et al., 2006, 2010; Antonioli et al., 2009a, b). During the Last Glacial Maximum (LGM, upper MIS 3 and MIS 2), about 30-19 cal. kyr BP (Lambeck & Purcel, 2004; Clark et al. 2009), and in particular at its end, the sea level is about 120–130 m lower than today in the Mediterranean Sea (Fig. 1c). After an initial slow rise (about 5 mm/yr), between 19 and 16 cal. kyr BP, sea level rises rapidly (on average 15 mm/yr) up to about 9 cal. kyr BP (Lamberck et al., 2002; 2014), and then progressively decreases as documented in the whole Mediterranean area (e.g. Boyer et al., 2005; Lamberck et al., 2011). From 6 cal. kyr BP the sea level decreases less than 1 mm/yr, approaching a relatively stable position (Lamberck et al., 2011; Vacchi et al., 2018).

From the geomorphological point of view the coastal morphogenetic processes are the most evident ones in the EI; however, due to the frequent high relief, fluvio-denudational and gravitational processes are both well developed. The coastal cliffs, 10 to more than 100 m high, are the most common coastal landforms. They surround most of the island and are subject to continuous retreat due to the wave erosion. Sandy and gravelly beaches are rather common and each one can be quite long, such as the Magazzini-Schiopparello (~2.0 km), Marina di Campo (~1.5 km), Procchio and Lacona (~1 km) beaches (Fig. 1a, b). In these localities, the backshore commonly hosts Holocene foredune systems (D'Orefice & Graciotti, 2018), fixed in place by vegetation and recently intensely anthropized. At the rear of the dunes system, coastal lagoons were sometimes present in the Holocene, with an extension of about 1 km onland (e.g. the tract of Mola-Capoliveri; Fig. 1a) (Bortolotti et al., 2015; Principi et al., 2015a, b; D'Orefice & Graciotti, 2018). More ancient systems of coastal dunes (bioclastic quartz-arenites) outcrop in several sites along the coasts of the eastern-central EI (Fig. 2a). These deposits formed during lowstand sea level which were related to the cold MIS 4 and MIS 2 (D'Orefice et al., 2007; D'Orefice & Graciotti, 2008). Fluvio-denudational landforms are predominantly erosional, as in the case of valleys, small valleys, gullies, gorges, sheet erosion landforms, ridges and, to a lesser extent constructional landforms which include the gently seawards-dipping alluvial and coastal plains in the eastern-central EI (Magazzini, Schioparello, San Giovanni, Fosso della Valdana-Mola, San Martino, Lacona, Campo nell'Elba,

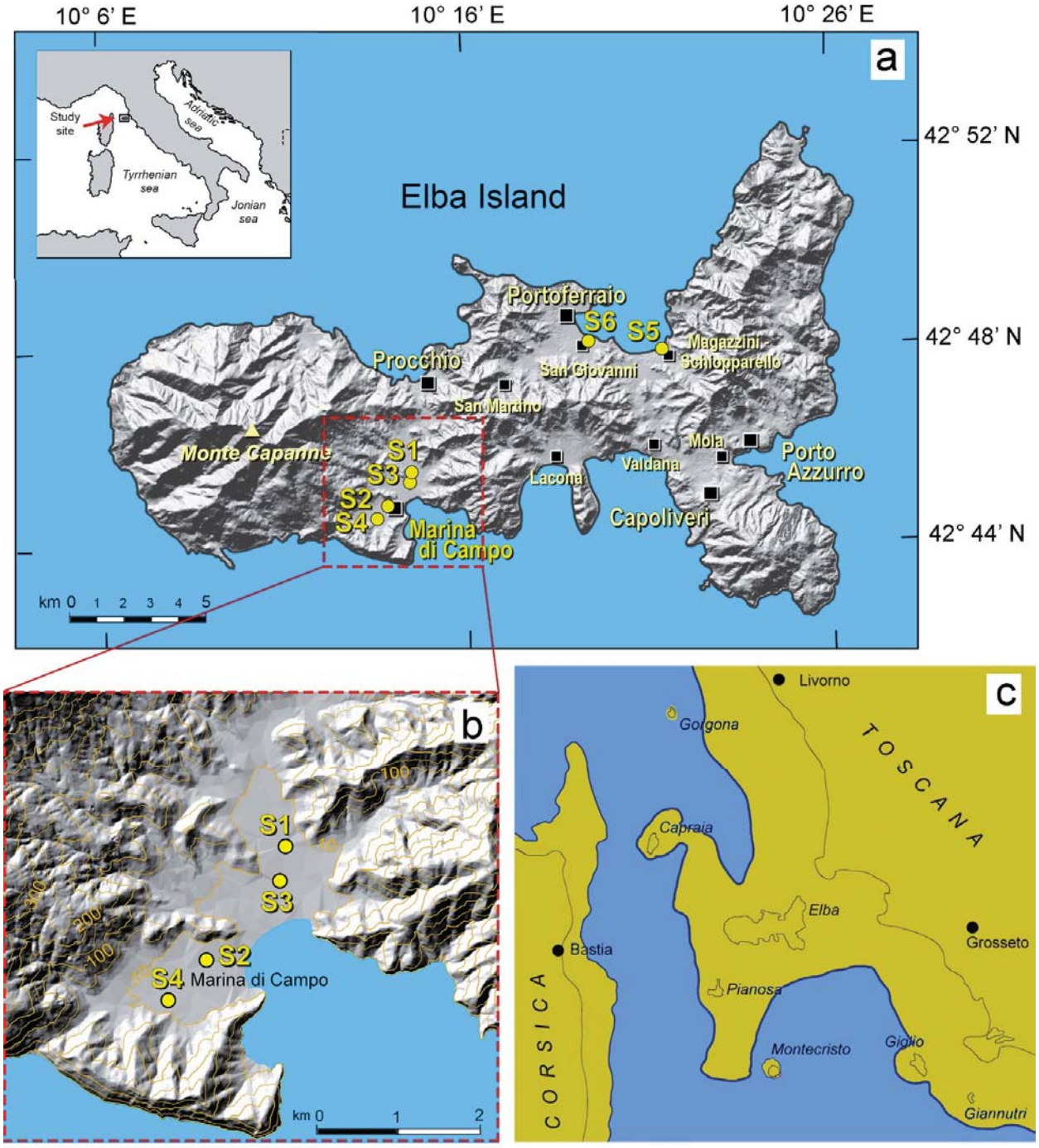

Fig. 1 - a) Geographical location of the Elba island and the six boreholes (S1÷S6) drilled by ISPRA in the frame of the Geomorphological Sheet "Isola d'Elba" at 1:50,000 scale (D'Orefice & Graciotti, 2018; ISPRA-Servizio Geologico d'Italia, 2018). S1÷S4 boreholes are the object of the present contribution. b) Zoom map of the Marina di Campo area. c) Paleogeographic scheme of the northern Tyrrhenian area during the LGM. In this period the sea level was lower, compared today, of about 120-130 m and the Elba-Pianosa Ridge was completely emerged and connected to the mainland through a wide corridor.

Porto Azzurro; Fig. 1a). Foothill zones, where strips of colluvial deposits put in connection the reliefs with the low lying alluvial plains, are also widespread. Landforms due to gravitational processes along slopes are expressed by degradation scarps, rockfalls, rotational landslides and, less frequently, flow landslides. The Monte Capanne (Fig. 1a) slopes are frequently covered by debris deposits (D'Orefice & Graciotti, 2018).

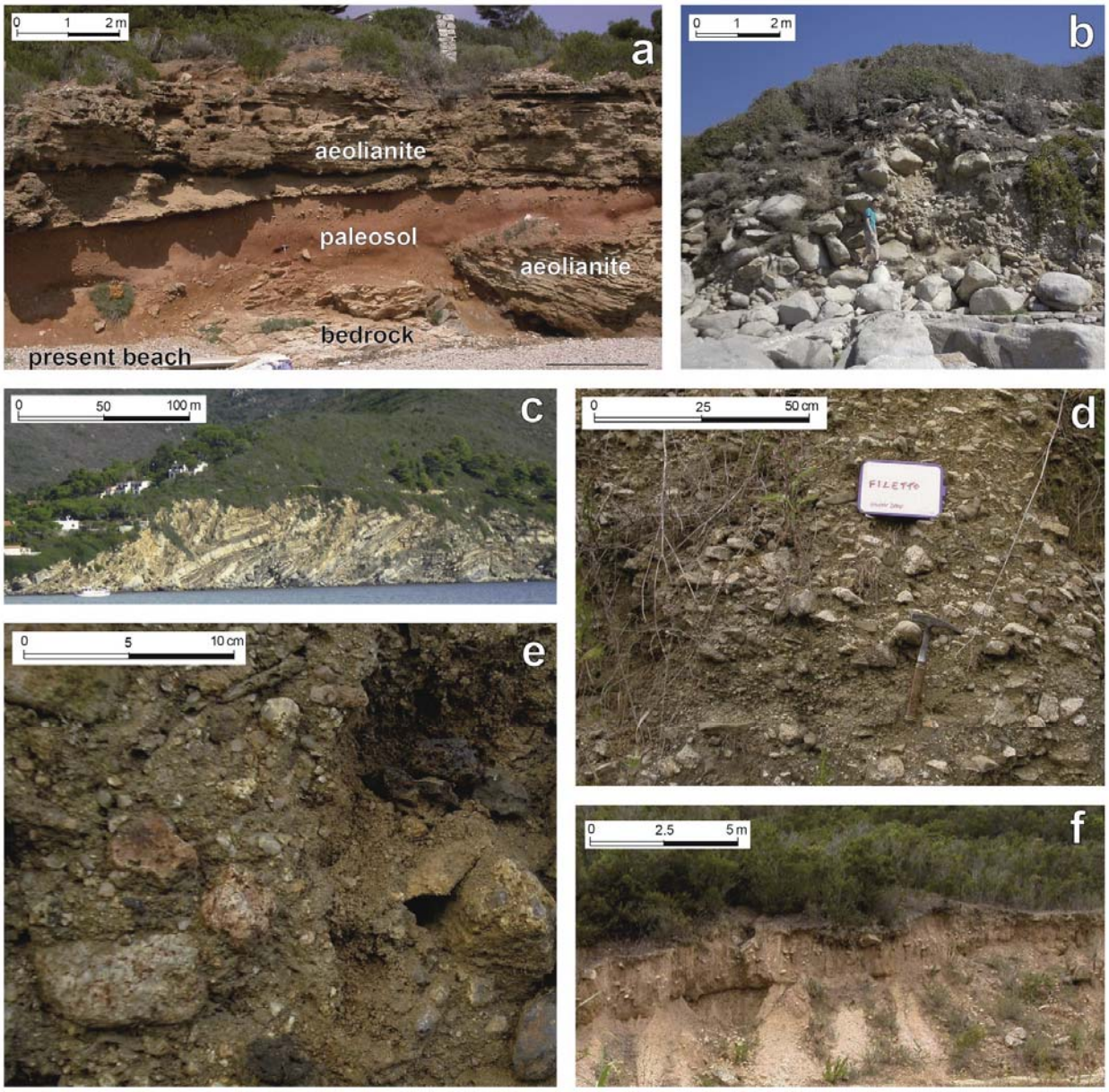

Fig. 2 - a) Aeolian bioclastic quartzarenites outcropping between Punta Barabarca and Stecchi (Capoliveri, eastern Elba Island; Fig. 1) at a distance of about 10 m from the present coastline; the two sedimentary bodies are separated by a paleosol (modified from D'Orefice & Graciotti, 2015). b) Debris flow deposit at the foot of the Monte Capanne western slope (Elba Island west coast). c) Turbidites belonging to the Marina di Campo Formation (Upper Cretaceous), outcropping along the north-eastern coast of the Campo Gulf. The bedrock is affected by evident folds. d) Upper Pleistocene terraced fluvial deposits outcropping in the Filetto Valley (NE of Marina di Campo). e) Iron slags within Holocene fluvial sediments outcropping in the final stretch of the Literno Valley (northern sector of the Marina di Campo plain). f) Colluvial deposits outcropping near the Filetto Valley (NE of Marina di Campo).

---------- -->>>>>

Fig. 3 - Simplified geological map of the Marina di Campo plain, broadly included in the municipal area of Campo nell'Elba. Legend: 1) colluvial deposits (Holocene); 2) fluvial deposits (Holocene); 3) aeolian deposits (Holocene); 4) beach deposits (Holocene); 5) lagoon and/or palustrine deposits (Holocene); 6) landslide and slope deposits (Upper Pleistocene - Holocene); 7) terraced fluvial deposits (Upper Pleistocene); 8) porphyry dikes and laccoliths (San Martino and Orano porphyries - Upper Miocene); 9) Monte Capanne monzogranite and thermo-metamorphic aureole (Upper Miocene); 10) calcareous siliciclastic turbiditic sequence (Marina di Campo Formation - Upper Cretaceous); 11) landfill and quarries; 12) debris flow fan; 13) alluvial fan; 14) mechanical continuous-core borehole; 15) hand-auger borehole. (Modified from D'Orefice & Graciotti, 2018).

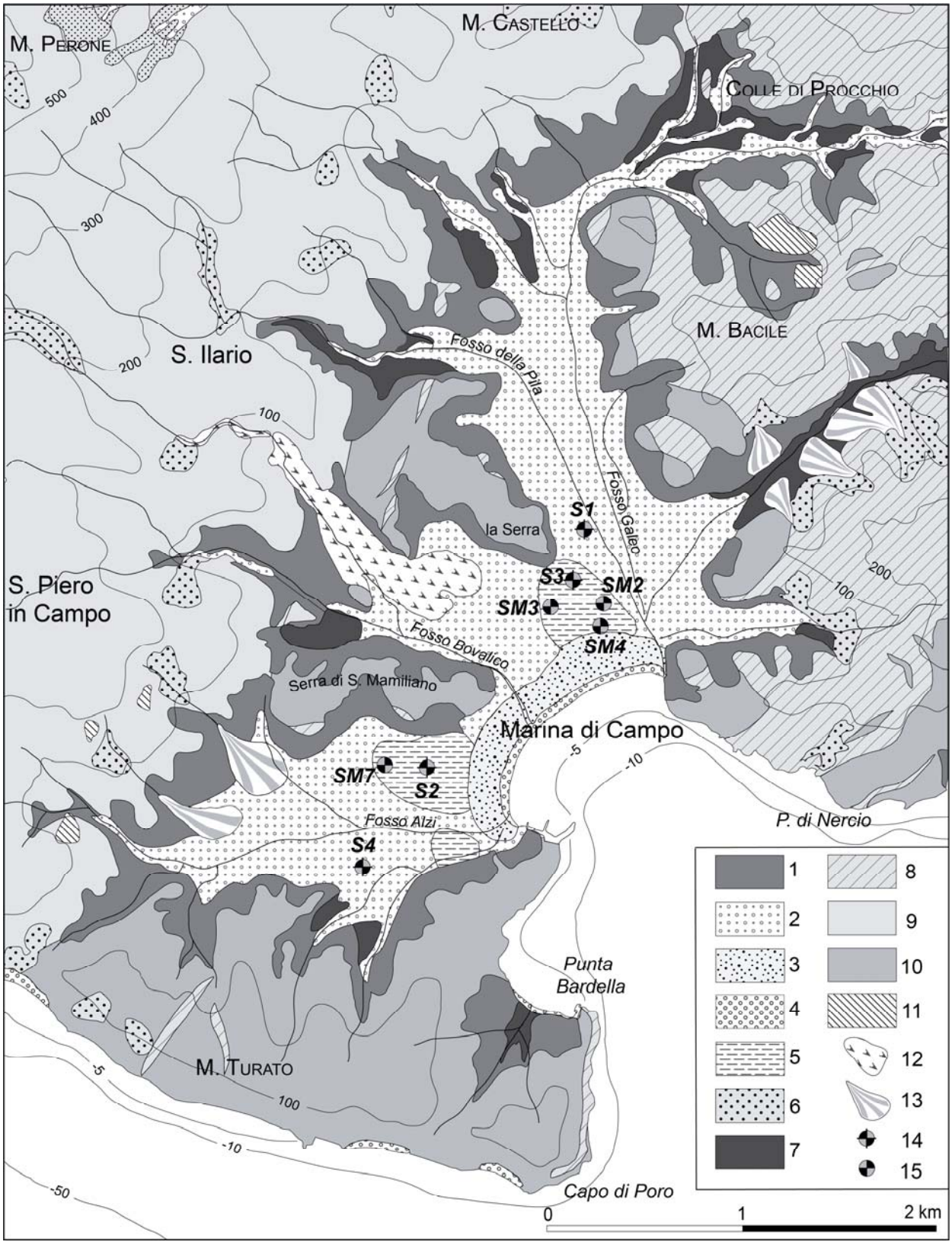
M. Perone
M. Castello
Colle di Procchio
M. Bacile
S. Ilario
Fosso della Pila
Fosso Galeo
la Serra
S. Piero
in Campo
Fosso Bovalico
Serra di S. Mamiliano
Marina di Campo
P. di Nercio
Fosso Alzi
Punta
Bardella
M. Turato
Capo di Poro
S1
S2
S3
S4
SM2
SM3
SM4
SM7
500
400
300
200
100
-5
-10
-50
0
1
2 km
1
2
3
4
5
6
7
8
9
10
11
12
13
14
15

2.1. Geology and geomorphology of the Marina di Campo area

The Marina di Campo plain is at the junction between the western and central part of the EI (Fig. 1a). The westernmost portion of the EI appears to have a three-dimensional hemispheric dome shape, pseudo-circular in plan. Such morphology is due to the Monte Capanne monzogranitic plutonic mass and its thermo-metamorphic aureole. The Monte Capanne (1,018 m a.s.l.) is characterized by rugged mountain terrain with rocky crests, peaks, steep slopes and deep valley often affected by debris-flow phenomena (Fig. 2b). Instead, the central sector of EI is characterized by modest elevation reliefs (<400 m), internally separated by flared and shallow valleys drained by short brooks. The hill-like reliefs in the westernmost part of this sector are formed by Marina di Campo Formation (Fig. 2c) which consists of Upper Cretaceous arenaceous-conglomeratic and calcareous-marly-arenaceous turbidites belonging to the Ripanera tectonic unit (Bortolotti et al., 2015; Principi et al., 2015a, b). The Marina di Campo Formation is intruded by dykes and laccoliths, frequently with porphyric texture, and acid in composition, emplaced in different time, ranging from 8 Ma (San Martino porphyry) to ca. 6.8 Ma (Orano porphyry) (Fig. 3). The Ripanera tectonic unit is separated by the Monte Capanne thermo-metamorphic aureole by means of a high-angle, east-dipping normal fault, named after the localities of Colle di Palombaia-Procchio (Bortolotti et al., 2015; Principi et al., 2015a, b). Since this structure downthrows, towards the east, the Ripanera unit with respect to the Monte Capanne thermo-metamorphic district, it is probably responsible for the formation of the Marina di Campo alluvial plain.

Fig. 4 - Frame n. 4105 of the "RAF fund" kept at the ICCD-Aerofototeca Nazionale. The photo, south oriented, was taken on January 2, 1944 on the Campo Gulf. It shows the Holocene dune system parallel to the coastline and the coastal plain behind, once occupied by ancient lagoons (a: Albarelli; b: Stagno; c: La Serra). These lagoons, partly included in the photo, are highlighted with oblique red striped (authorization to use for editorial purposes on the part of ICCD - MiBACT and the British School at Rome - further reproduction and/or duplication by any means is prohibited).

The Marina di Campo plain is interrupted by two rock spurs (Serra di Mamiliano and La Serra), which are isolated outcrops of the Marina di Campo Formation. These spurs divide the plain into three wide valleys (widths between 500 and 700 meters), gently dipping towards the Campo Gulf, where the Alzi, Bovalico and Pila-Galeo streams debouch (Fig. 3).

Late Quaternary continental deposits outcrop in the valley floors and in the foothills of the surrounding reliefs, and they gradually pass seawards to coastal-marine sediments.

The continental deposits are essentially represented by Upper Pleistocene and Holocene alluvial sediments. The most ancient alluvial deposits are incised and terraced by the Holocene drainage network and, accordingly, no longer affected by the current fluvial dynamics. They are basically relict fluvial plains whose uppermost depositional surfaces are at 10-15 m above the present sea level (D'Orefice & Graciotti, 2018). Such surfaces are the top of sedimentary bodies, sometimes more than 10 m-thick, constituted by heterometric, poorly rounded pebbles, heterogeneous in composition and largely immersed in a brown-reddish sandy to silty matrix (Fig. 2d). Conversely, the most recent fluvial deposits are composed of finer granulometries, such as silts, sands and fine-grained, poorly sorted and subangular gravels. Embedded in such deposits, angular metal clasts (slags), pluri-centimetric in size, can be found, probably reflecting the remains of the metallurgic fusion of the iron minerals during the Etruscan, Roman and Medieval times (Fig. 2e). The thickness of these deposits is variable and can locally exceed some meters (D'Orefice & Graciotti, 2018).

The fluvial deposits laterally pass into extensive and thick colluvial sediments (Fig. 2f) or small alluvial fans, as well as debris flow deposits.

In the littoral zone, lagoon and marshy deposits consisting of ultra-dark organic silty clays outcrop at shallow depth. These deposits suggest the presence of past coastal lagoons, developing behind the Holocene

dune systems of Marina di Campo, parallel to sandy beach ridge and bow-like shaped. More in detail, three separated fossil lagoons have been distinguished: the first one is between the camping area and the La Serra locality (northern sector of the plain), the other two are closely behind the inhabited area (Albarelli and Stagno localities) (Figs. 3 and 4). The real limit of the lagoon areas does not actually coincide with the one shown in Fig. 3, as it is downsized by the current river sedimentation. The marine sector, included in the Gulf of Campo, can be considered the underwater continuation of a pocket-beach, whose morphology closely follows the trend of the coast up to the isobath -50. Here the sea bottom, slightly sloping towards SE, is characterized, up to about 40 m below sea level, by sandy and gravelly Holocene deposits of HST, with a thickness between about 2 and 6 m (Principi et al., 2015b). These deposits pass to sandy pelites between -40 and -60 m. Below the isobath -60, under a limited Quaternary cover, a continental abrasion shelf modeled on ancient sediments develops (Principi et al., 2015b). This platform extends southward for about twenty kilometers.

3. MATERIALS AND METHODS

The geological and geomorphological mapping (1:10,000 scale) was supported by historical to recent bibliographic-cartographic literature, as well as by published scientific data, technical geological reports, geognostic investigations, multiscalar and multitemporal photo-interpretation.

The photo-interpretation was based on the flights: 1944-45 RAF (Britain Royal Air Forces), 1954-55 GAI (Italian Air Group), 1975, 1995, 1996, 1997, 1998 (Tuscany Region) and 1988-1989 (Italian photo aerial archives).

3.1. Drillings

Late Quaternary stratigraphy of Marina di Campo coastal plain was reconstructed by means of four continuous mechanical coring performed by crawler drill rig of General Trivel Company (boreholes S1-S4; Φ 101 mm), down to 23-25 m below the ground surface (BGS). Four additional surface boreholes (SM2, SM3, SM4 and SM7), 3.20 to 4.10 m BGS, were also performed with a manual auger.

The recovered sedimentary successions were submitted to sedimentological, biostratigraphical (foraminifers, malacofauna and palynology) analyses, as well as AMS dating.

Analyses have been carried out mainly on the S1 and S2 cores because of their appreciable lithological variability and the relatively higher micro-macrofaunistic and pollen content. Such features assure on the possibility to reconstruct the various sedimentary paleoenvironments in the study area.

3.2. Grain size analysis

Quantitative and qualitative granulometric analyses were processed. The quantitative analysis (35 samples: 14 from the S2 core and 21 from S3 core) of the coarser fraction (>0.074 mm) was determined by wet sieve technique, while the finest one was determined by densitometry technique. The samples were classified according to the criteria of the Italian Geotechnical Association (AGI, 1977).

3.3. Micropaleontological assemblages

96 samples (46 from S2 core and 52 from S3 core) were analysed at the Micropaleontological Laboratory of the University of Siena for macro- and micropaleontological contents, paying particular attention to the foraminiferal assemblages. Samples were prepared with classic washing technique (Green, 2001 and reference therein): sediment samples were dried and weighed (weighs vary from a minimum of ~100 g to a maximum of ~400 g), sieved in water over a 63 μm sieve, then dried in oven. To facilitate the analyses, the fraction >2 mm was observed separately. Both preparation and sample analyses were performed from the stratigraphic top to bottom.

3.4. Palynology

Palynological analysis was carried out on 28 samples from the two cores having more favorable lithologies (i.e. clay, rich-organic clay, silt) and a good chronological frame i.e. S2 and S3. The samples (14 from S2 and 14 from S3 cores) were processed at the Palynological Laboratory of the University of Florence, according to standard chemical-physical procedures which main steps are below specified. Following the addition of one *Lycopodium* tablet to determine palynomorph concentrations, samples, each weighing 10 g, were treated with HF, HCl, sodium hexametaphosphate, KOH, zinc chloride separation (density solution at 2.0). Residues were then sieved in an ultrasonic bath using a 10 mm polymer mesh. Mobile slides were mounted using glycerol and analysed using optical microscopes.

3.5. Radiocarbon dating.

29 samples from S1, S2, S3 and SM4 cores were dated by Accelerator Mass Spectrometry (AMS) in both the laboratories at CEDAD (Salento University) and at INFN-LABEC (Florence; Fedi et al., 2007). Datings were carried out on samples including microfossil shells, charcoals and other vegetal remains. Before any chemical treatment, the collected samples were observed under the optical microscope to identify possible macroscopic contaminants. Charcoals and vegetal remains were treated according to the so-called Acid-Base-Acid (ABA) procedure, in order to remove possible contaminations by carbonates and humic substances. Carbon was then extracted from the cleaned samples as CO_2 by acidification, in the case of shells, or by combustion, in the case of charcoals and other organic materials. In both laboratories, graphite pellets for the AMS measurement were obtained by reaction of CO_2 with H_2, in the presence of iron as catalyst. $^{14}C/^{12}C$ isotopic ratios measured in the unknown samples were corrected for background counts and for isotopic fractionation, by measuring the $^{13}C/^{12}C$ isotopic ratios in the accelerator beam line too. IAEA-C6 sucrose and NIST Oxalic Acid II were used as primary standards for normalization purposes in case of samples measure at CEDAD and at INFN-LABEC, respectively.

According to the international agreement, the measured conventional radiocarbon ages are shown as

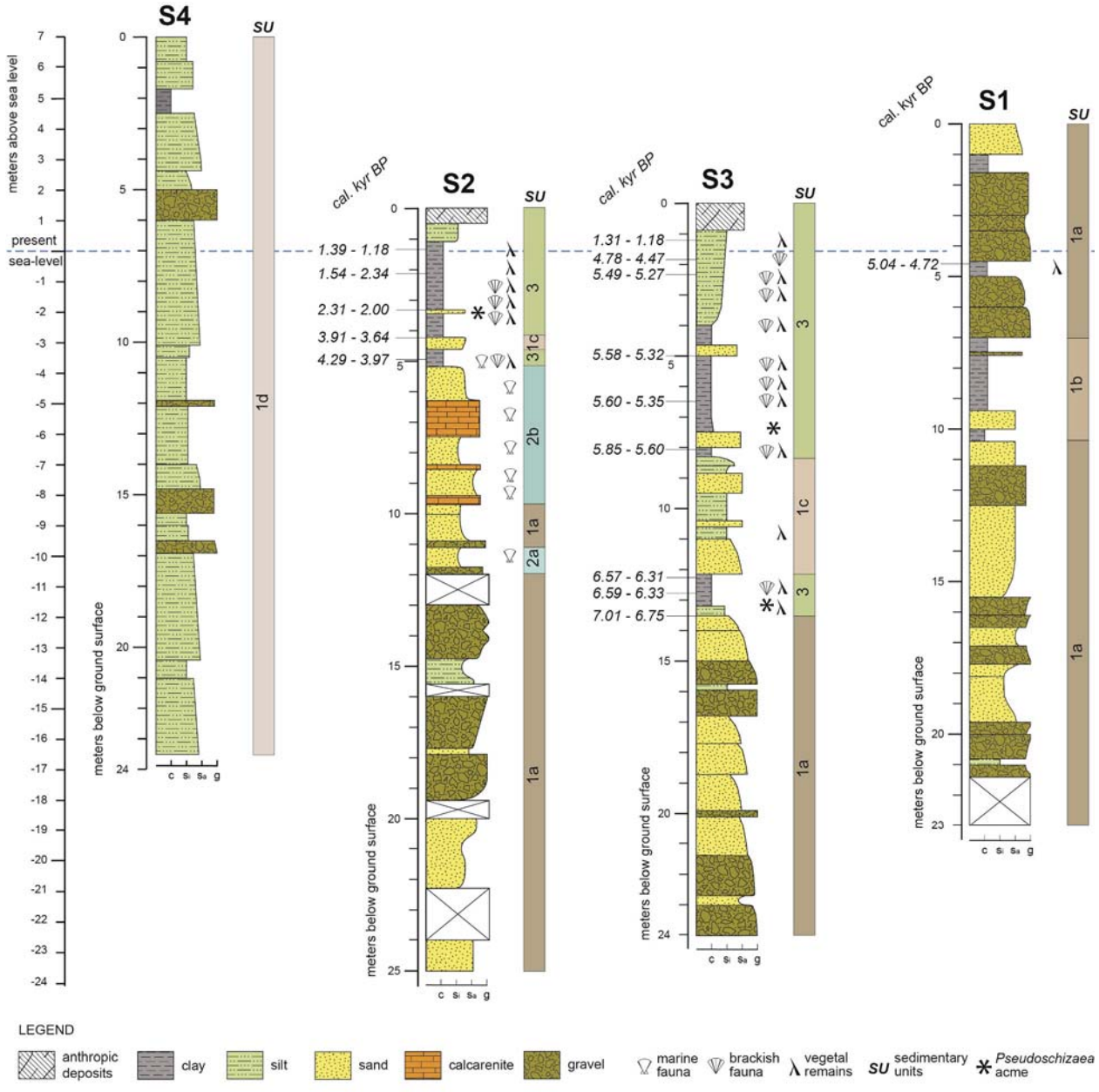

Fig. 5 - Stratigraphic logs of the cores recovered in the Marina di Campo coastal plains (Campo nell'Elba Municipality) according to a SW-NE transect. For the description of the sedimentary units and subunits see the text at 4.1.
S1: N42°45.420' E10°14.414' (La Pila); S2: N42°44.735' E10°13.821' (near the school of Marina di Campo); S3: N42°45.235' E10° 14.374' (La Serra); S4: N42°44' 27.03'' E10°13' 35.68" (Albarelli).

years Before Present (BP). Calibration has been performed following the IntCal13 and Marine13 calibration curves (Reimer et al., 2013) and using OxCal software, v.4.3 (Bronk Ramsey, 2009). In the case of samples collected from S2 and S3 cores, calibration was performed using a Bayesian approach, i.e. considering what we *a priori* knew about the samples relative chronology as inferred from the stratigraphy (Bronk Ramsey, 2008; Bronk Ramsey & Lee, 2013). The P_Sequence algorithm was applied for the calibration to consider also the possible variability in sedimentation rate.

4. RESULTS

4.1. Borehole lithostratigraphy

S1 borehole

It covers 23 m BGS (between 4.00 and -19.00 m a.s.l.) (Fig. 5). The 23.00 to 10.40 m BGS interval includes a well stratified alternation of gravel and silty sand (sometime weakly gravelly). The generally hetero-

metric, heterogeneous, subangular and often reversely graded gravels have an open-work texture in the basal 1.60 m (between 23.00 and 21.40 m BGS). The interval between 10.40 and 7.00 m BGS is mainly formed by greyish silty clay weakly sandy, with ocher colour streaks and thin intercalation of fine-grained gravel. Two coarser-grained beds intercalate in the silty clay: the first one (between 10.00 and 9.40 m BGS) is composed of silty-clayey sand with ocher colour streaks; the second one (7.60÷7.55 m BGS) is composed of fine-grained gravels. The succession, predominantly formed by gravels between 7.00 and 1.60 m BGS, is interrupted by a dark silty clay stratum containing vegetal remains, between 5.00 and 4.50 m BGS. Gravels are generally fine-grained, heterogeneous and supported by a silty-sandy matrix. The gravels pass, between 1.60 and 1.00 m BGS, to a silty clay weakly gravelly. The core ends at the top with one meter of brown silty sand weakly gravelly.

S2 borehole

S2, from 1.29 m a.s.l., reached the maximum depth of 25.00 m BGS (-23.71 m a.s.l.) (Fig. 5). The interval from 25.00 to 11.90 m is characterized by gravel beds alternating with prevalently silty clayey sand beds. Gravels, supported by a sandy-silty matrix, are heterometric (from few mm up to 8 cm in diameter), heterogeneous (clasts from monzogranitic, porphyritic and arenaceous lithotypes) and subangular. The gravelly strata may exhibit a reverse grading, while the finer beds are sometimes characterized by oxidized sandy laminae. The gravelly strata reach a thickness of 150 cm on average, while those consisting of silty clayey sand have thicknesses between 20 cm and 230 cm. A sharp erosive contact separates this interval from the overlying one.

The interval between 11.90 and 11.10 m BGS is formed by fine sand weakly silty and clayey with tiny fragments of marine shells. The interval between 11.10 and 9.70 m BGS includes, at the base, a 20-cm thick gravel level rich in siliceous and poorly elaborate centimetric clasts in fine matrix. The gravels are in their turn overlain by a laminated silty clayey sand with ocher speckles, passing upwards to fine sand with clayey silt having a total thickness of 120 cm. Between 9.70 and 5.20 m BGS fossil-rich strata are present. They consist of sand, silty clayey sand and sand with clayey silt, alternating with three biocalcarenites strata: the first one between 9.70 and 9.40 m, the second one between 8.50 and 8.40 m and the third one between 7.50 and 6.30 m. Between 5.20 and 1.10 m BGS, plastic organic clay with sandy silt, dark gray in color, predominate. The contact with the underlying deposits is sharp. The continuity of this clayey interval is interrupted, in its lower portion (between 4.35 and 4.65 m BGS), by sand (mainly of carbonate composition and whitish color from 4.65 to 4.60 m BGS) with clayey silts and, in the central portion (from about 3.30 to 3.45 m BGS), by sand with clayey silt weakly gravelly. In the organic clays are present up to about 1.60 m BGS, mollusks (unbroken or in fragments), and ostracods, while the remaining portion (between 1.60 and 1.10 m BGS) contains only vegetal remains. The sandy-clayey silt top interval (between 1.10 and 0.50 m BGS), is barren in mollusks and covered by 50 cm of landfill containing anthropogenic remains.

S3 borehole

S3, from 1.33 m a.s.l., reaches a maximum depth of 24.00 m BGS (-22.67 m a.s.l.) (Fig. 5).

The lower part, from 24.00 to 13.50 m BGS includes from the bottom: open-work and normally graded loose coarse gravels; silty gravelly sands weakly clayey; sands with clayey silts; sandy matrix-supported and normally-graded coarse and fine gravels; sands with weakly clayey silty gravels. This interval does not contain marine macro-fossil remains and presents many similarities with the basal part of S2 from the lithological, granulometric and textural point of view.

The 13.50÷12.15 m BGS interval consists, for the first 30 cm, of silt with sandy clay, overlain by 105 cm of very dark clay with sandy silt progressively richest in fossils upwards.

The 12.15÷8.30 m BGS interval mainly includes silty clayey sands, silts with sandy clays, clayey silty sands and clayey gravelly silts.

The interval 8.30÷4.00 m BGS is characterized by plastic organic clays (dark clays with sandy silts), passing upwards (from 4.00 to 1.80 m BGS) to a silt with clay weakly sandy.

The upper part, from 1.80 to 0.87 m BGS, consists of silts with clay weakly sandy, with abundant mollusks (up to 1.65 m BGS) and vegetal remains.

The last 0.87 m are characterized by the presence of sandy clayey silt weakly gravelly, affected by pedogenic and anthropogenic reworking processes.

S4 borehole

S4, from 7.00 m a.s.l., reaches a maximum depth of 23.50 m BGS (-16.50 m a.s.l.) (Fig. 5). It is a quite uniform succession, largely characterized by clayey sandy silts, frequently weakly gravelly, with intercalated silty clayey or sandy silty gravel beds (at 16.90÷16.50, 15.60÷14.80, 12.10÷11.90, 6.00÷5.00 m BGS intervals). A silty clay stratum with ocher speckles is present in the upper part, between 2.60 and 1.70 m from BGS.

Hand auger drillings

The manual drillings SM2 (max depth 3.20 m BGS) and SM4 (max depth 4.10 m BGS), include respectively from the bottom, about 0.20 m and 1.10 m of silt with clay weakly sandy, passing upwards to an alternation of silty clay and sand, at places coarse, which are 2 m (SM2) and 2.50 m (SM4) thick. At the top of both drillings is present a dark organic clay with silts, of variable thickness between 0.50 (SM4) and 1.00 m (SM2).

The manual drilling SM3 (max depth 3.50 m BGS) includes from the bottom: 0.20 m of blue-gray clays; 1.70 m of clayey silts alternate to coarse sands; 0.40 m of gray clay; 0.80 m of clayey silt with sand; 0.40 m of topsoil.

The manual drilling SM7 includes only 0.5 m characterized by the large occurrence of coarse anthropogenic remains.

The overall granulometric, textural and sedimento-

Sample Identifier	Core # (depth in core, m)	Material	Conventional ^{14}C age (yr BP)	Unmodeled Cal age (yr BP - 68% probability)	Unmodeled Cal age (yr BP - 95% probability)	$\delta^{13}C$ (‰, *vs.* SMOW)
LTL4781A	S1 (4.60)	vegetal remain *(C)*	4305 ± 50	4970 – 4830	5040 – 4720	-28.1 ± 0.3
LTL15769A	S2 (1.35)	charcoal *(W)*	1395 ± 45	1350 – 1280	1390 – 1180	-24.4 ± 0.6
LTL5655A	S2 (1.46)	charcoal *(W)*	not datable	–	–	–
Fi3253 (S2_5)	S2 (2.10)	charcoal *(W)*	1540 ± 45	1530 – 1380	1540 – 1340	-25.7 ± 0.5
LTL15770A	S2 (2.25)	charcoal *(W)*	923 ± 45	910 – 790	930 – 740	-29.7 ± 0.7
Fi3235/37 (A_14)	S2 (2.54)	wood *(W)*	205 ± 30	modern		-27.7± 0.9
LTL15771A	S2 (3.33)	vegetal remain *(W)*	2152 ± 45	2310 – 2060	2310 – 2000	-22.6 ± 0.5
LTL4782A	S2 (4.30)	shell *(L)*	3830 ± 45	3850 – 3700	3910 – 3640	-17.0 ± 0.3
LTL4783A	S2 (4.95)	shell *(L)*	4090 ± 45	4220 – 4070	4290 – 3970	-4.1 ± 0.3
LTL4914A	S2 (6.50)	shells *(M)*	35240 ± 400	39800 – 38890	40290 – 38550	-2.8 ± 0.5
LTL8222A	S2 (7.20)	benthonic foraminifer *(M)*	27160 ± 200	31070 – 30800	31200 – 30640	-9.5 ± 0.2
LTL8283A	S2 (7.20)	ostracod *(M)*	22315 ± 200	26350 – 25930	26630 – 25790	-7.7 ± 0.2
LTL5656A	S2 (8.50)	shell *(M)*	not datable	–	–	–
LTL5657A	S2 (9.40-9.70)	shell *(M)*	39255 ± 800	43410 – 42210	44330 – 41800	-16.3 ± 0.5
LTL4784A	S2 (10.90)	organic matter *(C)*	not datable	–	–	–
LTL5658A	S2 (11.30)	shell *(M)*	33120 ± 200	36910 – 36320	37460 – 36160	-12.5 ± 0.5
LTL16443A	S3 (1.20)	charcoal *(W)*	1336 ± 30	1300 – 1190	1310 – 1180	-23.4 ± 0.4
LTL4927A	S3 (1.80)	shell *(L)*	4430 ± 40	4680 – 4520	4780 – 4470	-8.8 ± 0.5
LTL4786A	S3 (2.35)	shell *(L)*	5020 ± 45	5430 – 5310	5490 – 5270	-3.6 ± 0.5
LTL16444A	S3 (2.57)	charcoal *(L)*	4534 ± 40	5310 – 5060	5320 – 5040	-31.4 ± 0.2
LTL5752A	S3 (3.90)	shell *(L)*	5830 ± 40	6720 – 6560	6740 – 6500	-3.1 ± 0.5
LTL5753A	S3 (5.00)	shell *(L)*	5105 ± 45	5560 – 5430	5580 – 5320	-7.8 ± 0.5
LTL5754A	S3 (5.75)	shell *(L)*	4290 ± 45	4960 – 4820	5030 – 4710	-1.8 ± 0.5
LTL5755A	S3 (6.50-6.60)	shell *(L)*	5140 ± 45	5570 – 5460	5600 – 5350	-3.2 ± 0.6
LTL4787A	S3 (8.10)	shell *(L)*	5350 ± 45	5770 – 5630	5850 – 5600	-6.2 ± 0.5
LTL4788A	S3 (12.20)	shell *(L)*	6025 ± 45	6510 – 6380	6570 – 6310	-6.1 ± 0.2
LTL4789A	S3 (12.80)	shell *(L)*	6035 ± 45	6520 – 6390	6590 – 6330	-4.4 ± 0.5
LTL12480A	S3 (13.52-13.60)	charcoal *(C)*	6040 ± 45	6950 – 6800	7010 – 6750	-31.3 ± 0.6
LTL8278A	SM4 (4.00)	organic clay *(L)*	not datable	–	–	–

Tab. 1 - Results of radiocarbon (^{14}C) dating. C = sample of continental environment; W = sample of freshwater wetland environment; L = sample of brackish lagoon environment; M = sample of marine environment.

logical characteristics and subordinately the macrofossiliferous content (mollusk shells, vegetal remains, etc.) of S1-S4 and SM2-4-7 cores permitted to describe 3 main sedimentary units (Units 1 ÷3) organized in 6 subunits (1a, b, c, d, 2a and 2b). The main features of these sedimentary units (SU) are shortly described as follows and shown in Figure 5:

- SU 1a consists of an alternation of heterometric, heterogeneous, subangular gravel beds with prevalently silty clayey sand beds, sometimes characterized by oxidized sandy laminae.
- SU 1b is composed of greyish silty clay weakly sandy, with ocher colour streaks and thin intercalation of fine-grained gravel.
- SU 1c consists of an alternation of silty clayey sands, silts with sandy clays, clayey silty sands and clayey gravelly silts
- SU 1d is composed of clayey sandy silts, frequently weakly gravelly, with intercalated silty clayey or sandy silty gravel beds.
- SU 2a consists of fine sand weakly silty and clayey with tiny fragments of marine shells.
- SU 2b consists of fossil-rich sand, silty clayey sand and sand with clayey silt, alternating with biocalcarenites strata.
- SU 3 is mainly characterized by dark plastic organic clay with sandy silt, passing upwards to a silt with clay weakly sandy; mollusks, ostracods and vegetal remains are abundant.

4.2. Geochronology

The results of radiocarbon (^{14}C) measurements are summarized in Table 1. In S2, datings of LTL4914A (6.50 m BGS; 35,240 ±400 yr BP) and LTL4783A (4.95 m BGS; 4,090 ±45 yr BP) samples suggest an interval of ca. 30 kyr in solely 1.5 m of sediments. This evidence could be interpreted either as due to the occurrence of a hiatus or the intervention of environmental factors causing non-accurate radiocarbon dates for shells (e.g.

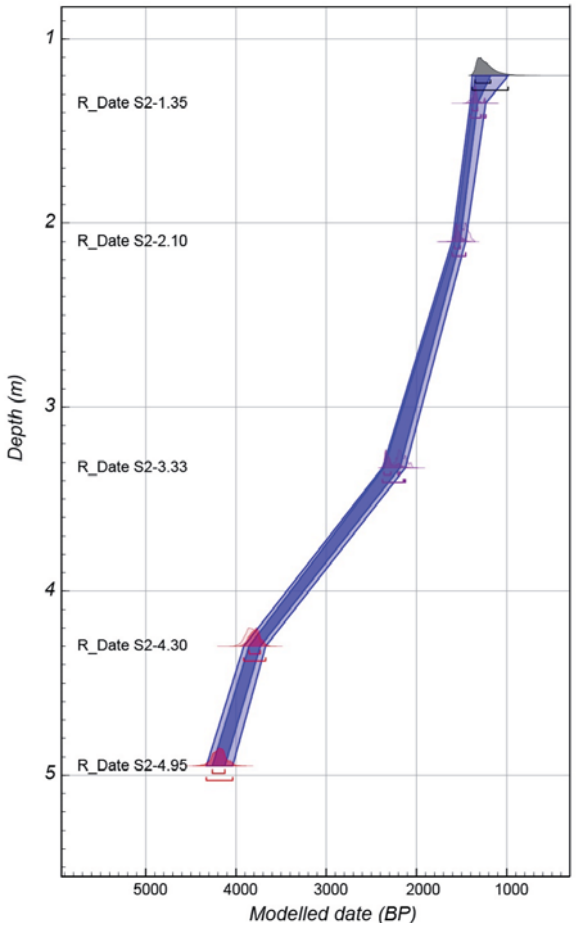

Fig. 6 - Age-depth profile of core S2, as obtained after running the P_Sequence model in OxCal. *A posteriori* distributions of probability for calibrated ages are reported using different colours according to samples origin, either marine or terrestrial.

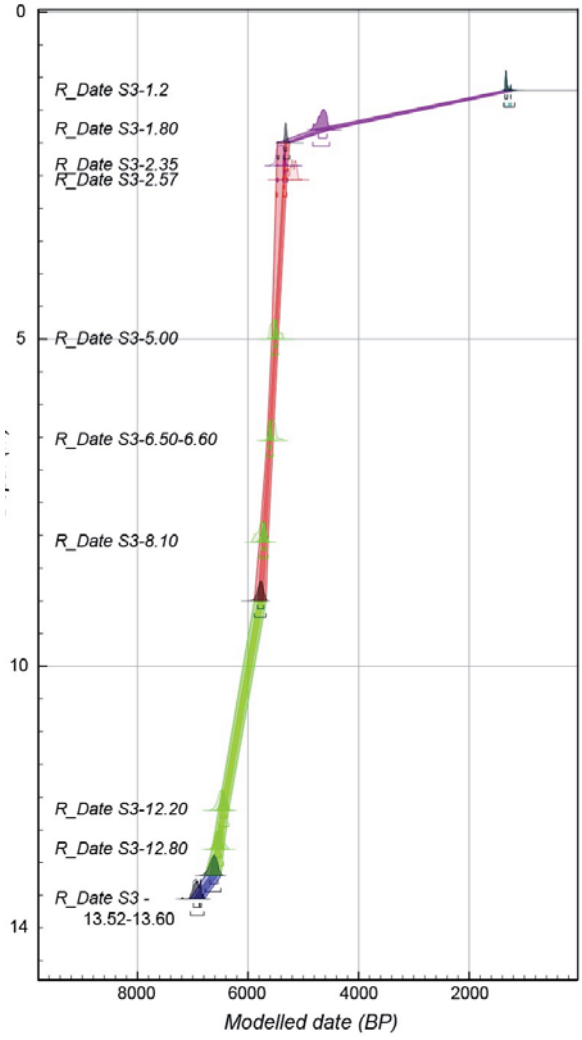

Fig. 7 - Age-depth profile of core S3, as obtained after running the P_Sequence model in OxCal. A posteriori distributions of probability for calibrated ages are reported using different colours according to samples origin, either marine or terrestrial. Different colours are also used to highlight the different average sedimentation rates along the whole core.

Gischler et al., 2008; Douka et al., 2010). The first hypothesis (i.e. a hiatus) was discarded, because the occurrence in the S2 strata of some specimens of the pink morphotype of *Globigerinoides ruber* (*G. ruber rosea*, see section 4.3). This taxon, recorded from the Upper Pleistocene, shows significant percentages only during interglacial phases (during MIS 5 and MIS 1). Lagoon sediments in S2 were deposited in continuity of sedimentation over the marine deposits of the submerged beach (from which come the specimens of *G. ruber rosea*) stratigraphically referable to the MIS 1 interval. Such stratigraphical attribution is in apparent contrast to the datings ranging between about 39 and 22 kyr (Tab. 1). The second hypothesis seems more likely. Indeed, the continental waters (river input), enriched with inorganic carbon coming from the limestones of the Marina of Campo Formation, could have mixed with the marine-coastal ones (i.e. lagoons). Recrystallization of carbonates, i.e. the incorporation of secondary $CaCO_3$ from the external environment needs also to be considered. The measured ages of the older shell samples do not fit with the relative chronology inferred from the stratigraphy: this can be interpreted as a further suggestion of problematic radiocarbon dating. In the upper part of S2, both marine and terrestrial samples can be organized in a coherent stratigraphical succession, with the exception of samples LTL15770A (2.25 m BGS; 923 ±45 yr BP) and Fi3235/37 (2.54 m BGS; 205 ±30 yr BP) (Fig. 6). In particular, the very young age of the charcoal sample LTL15770A and in particular of the wooden sample Fi3235/37 can be due to an infiltration phenomenon by modern material, probably roots.

In S3 three samples, LTL16444A (2.57 m BGS; 4,534 ±40 yr BP), LTL5752A (3.90 m BGS; 5,830 ±40 yr BP) and LTL5754A (5.75 m BGS; 4,290 ±45 yr BP), appear as outliers. Figure 7 shows the probability density functions of calibrated ages as calculated after excluding these samples: the sequence spans several

S2 Borehole						Vegetals			Mollusks				Other taxa							Benthic Foraminifera														Planc. Foram.		
Biofacies interval	Sample/High (m)	Dry weight (g)	Fraction > 2 mm (g)	Fraction 63 µm - 2mm (g)	Fraction > 63 µm %	Carbonized remains	Characeae oogons	*Ruppia* (fruits)	*Cerastoderma glaucum*	*Abra ovata*	*Hydrobia* sp.	Undetermined taxa	Non-ornamented ostracods	Ornamented ostracods	Serpulids	Bryozoans	Calcareous Algae	Echinoid remains	Sponge spicules	*Ammonia tepida*	*Ammonia beccarii*	*Asterigerinata mamilla*	*Lobatula lobatula*	*Elphidium spp*	*Globulina gibba*	*Guttulina communis*	*Neoponides schreibersii*	*Nonion depressulum*	*Nubecularia lecifuga*	*Quinqueloculina spp*	*Rosalina spp.*	*Triloculina spp.*	*Textularia sp.*	*Globigerina bulloides*	*Globigerinoides spp.*	*Orbulina universa*
S2-F	S2-1.18-1.28	277,17	0,27	23,22	8,5%	C																														
S2-F	S2-1.48-1.58	193,20	1,16	19,99	10,9%	C	R						R?																							
S2-E	S2-1.80-1.88	195,69	5,91	80,24	44,0%	C	R																					R								R?
S2-E	S2-2.10-2.20	185,53	4,61	48,35	28,5%	C			R											R																
S2-E	S2-2.40-2.50	184,49	9,19	65,97	40,7%	C			R	R	R		R							R								R								
S2-E	S2-2.70-2.80	207,24	4,93	37,99	20,7%	C	A		R	R	R		R							R								R								
S2-E	S2-3.00-3.10	236,12	99,71	39,68	59,0%	C	R		R		R		R																							
S2-E	S2-3.33-3.43	228,86	106,34	51,86	69,1%	C																														
S2-E	S2-3.60-3.70	209,68	8,56	104,67	54,0%	C			R		R		R							R								R								
S2-E	S2-4.00-4.10	184,36	1,52	54,48	30,4%	C	R		R	R																										
S2-E	S2-4.30-4.40	252,80	6,95	117,50	49,2%	C		C	A	A	C		C							R								R								R
S2-E	S2-4.51-4.58	104,20	1,73	43,88	43,8%	C	R																													
S2.D	S2-4.60-4.66	112,60	13,51	72,45	76,3%	C	R					A	R	A			R	A	R		A	R	C	A	C					A	C				R	
S2.D	S2-4.84-4.94	166,51	4,68	67,16	43,1%	C			A	C	R	R	A				R	C			C		R	R	R			C	R	A		C				C
S2.D	S2-5.00-5.10	174,87	4,36	84,66	50,9%	C		R	C	C	R	C	C		R		C	A			C	R	C	C	C			C	R	A					R	
S2.D	S2-5.30-5.40	165,87	6,96	94,96	61,4%	C		C	C	C	C	A		A			C	C	R		A		C	A	R			R		C	C	C				
S2.D	S2-5.60-5.70	189,80	35,21	123,31	83,5%	R						A		A	C	R	A	C	R		C	R	C	C					C		R	A			R	
S2.D	S2-5.90-6.00	432,63	7,77	308,91	73,2%							A		C	C	R	A	C	R		A	C	R	C		R			C	A	C	A	R		R	
S2.D	S2-6.15-6.23	216,69	13,81	110,46	57,3%							A		C			A	C	C		A	R	C	A		R	C			A	C	A			R	R
S2.D	S2-6.90	196,38	50,82	128,31	91,2%							A		A	R	R	C	A	A		A	R	R	C						C	R				R	
S2.D	S2-7.20-7.25	240,89	101,68	99,81	83,6%							C		A			R	C	A		A	R	R	C			R	R		A	R			R	R	
S2.D	S2-7.55-7.60	188,28	79,15	66,59	77,4%							A						C	C		C						R			A	R					R
S2.D	S2-7.90-8.00	134,31	58,38	48,03	79,2%							C						C		R							C			A					R	R
S2.D	S2-8.15-8.25	233,24	28,08	156,00	78,9%							C							C								R			A					R	
S2.D	S2-8.70-8.80	189,50	48,03	126,66	92,2%							A		C		X		R	R		R		R	A			C			A						
S2.D	S2-9.00-9.10	198,32	4,00	131,48	68,3%							R		C		X		R	C		R		A	C			C			C	R	C			R	R
S2.D	S2-9.30-9.40	191,54	125,36	63,45	98,6%							A		C				C	C		A	C	R	A	R			R							C	R
S2.D	S2-9.55-9.60	141,99	120,56	16,36	96,4%							C		R		X		R	X		R			R												
S2-C	S2-9.80-9.90	269,44	2,11	163,19	61,3%																															
S2-C	S2-10.00-10.10	253,27	1,17	176,20	70,0%																															
S2-C	S2-10.40-10.48	250,07	0,00	71,24	28,5%																															
S2-C	S2-10.73-10.79	177,49	0,00	108,92	61,4%																															
S2-C	S2-10.90-11.00	228,31	10,61	163,37	76,2%							R?																								
S2-B	S2-11.18-11.26	130,75	0,97	123,74	95,4%													X	X			R						R		R		R				
S2-B	S2-11.70-11.75	167,09	0,14	147,28	88,2%							C	C			X		C	C		R		R	R						R						
S2-B	S2-11.83-11.90	126,38	0,15	98,12	77,8%							C									R	R		R						R						
S2-A	S2-13.20-13.25	226,56	69,62	103,51	76,4%																															
S2-A	S2-14.90-14.95	201,85	0,00	67,61	33,5%																															
S2-A	S2-15.40-15.45	162,05	0,46	46,59	29,0%																															
S2-A	S2-16.30-16.35	244,86	56,57	97,70	63,0%																															
S2-A	S2-16.70-16.75	165,31	0,00	92,92	56,2%																															
S2-A	S2-18.55-18.60	149,93	1,02	50,15	34,1%																															
S2-A	S2-19.20-19.25	268,23	3,96	102,76	39,8%																															
S2-A	S2-20.50-20.55	226,31	0,75	91,57	40,8%																															
S2-A	S2-21.25-21.30	270,49	16,00	137,35	56,7%																															
S2-A	S2-23.40-23.45?	135,20	1,35	40,41	30,9%	R?						R?																								

Tab. 2 - Results of the macro- and micro-paleontological analyses from the S2 borehole. Legend: A = abundant; C = common; R = rare; X = not estimated abundance; R? = not in place.

millennia, since the fifth millennium BC to the Early Middle Ages. Abrupt changes in the sedimentation rates (at least three) should be considered to obtain a satisfying agreement with the previous information.

4.3. Bioindicators

4.3.1. Observation from >63 µm washed residues

S2 borehole

Microfossils remains were first recovered from the interval between S2 11.83-11.90 and S2 11.18-11.26 (Interval S2-B in Tab. 2); they include mollusks, ostracods, bryozoans, serpulids, echinoids, sponge spicules, planktonic and benthonic foraminifers with common *Ammonia beccarii*, *Asterigerinata mamilla, Elphidium* spp. and *Quinqueloculina* spp. Microfossils are absent from the base of S2 core and in Interval S2-C (Tab. 2) from sample S210.90-11.00 and S2 9.80-9.90. An abundant and well-diversified fossiliferous fraction (mollusks, ostracods, serpulids, bryozoans, calcareous algae, echinoids, sponge spicules and benthic and planktonic foraminifers) is present in the sediments between sample S2 9.55-9.60 and sample S2 4.60-4.66 (Interval S2-D in Tab. 2). Among benthic foraminifers, the most common taxa are *Ammonia beccarii*, *Asterigerinata mamilla*, *Elphidium* spp., *Lobatula lobatula*, *Nubecularia lucifuga*, *Rosalina* spp., as well as several miliolid specimens of *Triloculina* and *Quinqueloculina* genera. Planktonic foraminifera, though rare, are represented by the species *Globigerina bulloides*, *Globigerinoides ruber*, *G. elongatus*, *G. trilobus* and *Orbulina universa*. Concerning the *Globigerinoides ruber*, it should be noted that the sample S2 7.20-7.25 from Interval S2-D contains some specimens of the pink morphotype (*G. ruber rosea*). From S2 5.30-5.40 m (upper part of Interval S2-D), significant changes in the assemblages are marked by the appearance of the genera *Cerastoderma glaucum*, *Abra ovata* and *Hydrobia* sp. among mollusks and by ostracods with a large number of non-ornamented speci-

S3 Borehole																	
							Vegetals		Mollusks			Other taxa			B. Foram.	
Biofacies interval	Sample/High (m)	Dry weight (g)	Fraction > 2 mm (g)	Fraction 63 µm - 2mm (g)	Fraction > 63 µm %	Microcrystalline gypsum	Carbonized remains	*Ruppia* (fruits)	*Cerastoderma glaucum*	*Abra ovata*	*Hydrobia* sp.	Non-ornamented ostracods	Resti di Pesci	Resti di insetti	*Ammonia tepida*	*Nonion depressulum*
S3-E	S3-0.93-1.00	163,78	1,14	20,98	13,51%		A									
	S3-1.20-1.25	169,35	2,33	35,56	22,37%		R									
	S3-1.50-1.55	161,50	0,16	10,85	6,82%		A	R								
S3-D	S3-1.80-1.85	123,50	0,45	3,71	3,37%	A	A		C	R	R	R			R	
	S3-2.10-2.15	105,90	0,65	4,77	5,12%	A	A		C	C						
	S3-2.35-2.40	187,91	4,52	10,25	7,86%	A	A	C	A	C	C	A	R		C	R
	S3-2.65-2.70	149,80	1,59	13,75	10,24%	A	C	R	C	R						
	S3-2.95-3.00	142,52	0,82	14,95	11,07%	A	C	R	R				R	R		
	S3-3.20-3.25	161,42	2,50	12,10	9,04%	A	A	R	A	C	R				R	
	S3-3.45-3.51	158,07	5,84	24,89	19,44%	A	A	R	A	C	C	R	R		A	R
	S3-3.72-3.80	166,55	2,67	17,89	12,34%	A	A	R	A	R		R	R	R		
	S3-4.00-4.08	100,05	1,03	4,73	5,76%	A	A	R	A	C	R	R				
	S3-4.30-4.35	166,53	4,26	57,76	37,24%		A		R	R	R					
	S3-4.55-4.60	221,62	6,32	109,52	52,27%		R									
	S3-4.80-4.88	280,20	54,06	114,80	60,26%		R									
	S3-5.05-5.12	135,01	5,19	13,94	14,17%	A	A	R	A	C	C	C	R		R	
	S3-5.30-5.35	84,40	0,18	3,99	4,94%	A	A	R	R			R				
	S3-5.60-5.70	132,64	2,66	22,30	18,82%	A	A	R	A	R	R	R	R		R	
	S3-5.95-6.00	123,96	1,62	16,04	14,25%	A	A	R	A	R	R	R				
	S3-6.30-6.36	118,97	0,32	12,75	10,99%	A	C	R	R	R	R			R		
	S3-6.58-6.65	121,45	3,48	26,21	24,45%	A	A	R	A	C	C	R	R		A	R
	S3-6.95-7.00	96,25	1,07	24,05	26,10%	A	A	R	A	C	C	R	R		C	R
	S3-7.10-7.15	182,80	2,75	69,87	39,73%	C	R		R	R						
	S3-7.35-7.40	164,28	4,98	77,85	50,42%		R		R	R						
	S3-7.65-7.70	193,74	18,75	85,06	53,58%		R		R	R						
	S3-7.95-8.00	214,20	13,17	82,83	44,82%		R		R							
	S3-8.10-8.18	135,08	1,11	13,51	10,82%	A	A	R	A	C	C	R				
	S3-8.40-8.46	239,99	13,89	120,59	56,04%		R		R							
S3-C	S3-8.65-8.70	77,09	0,60	12,78	17,36%											
	S3-9.10-9.16	287,60	2,36	191,96	67,57%				R?							
	S3-9.50-9.56	160,21	0,27	24,15	15,24%											
	S3-10.15-10.22	155,72	1,64	69,89	45,94%											
	S3-10.55-10.62	235,12	33,92	120,11	65,51%		R									
	S3-10.80-10.85	170,76	0,32	85,92	50,50%		R									
	S3-11.05-11.10	165,21	21,70	108,60	78,87%											
	S3-11.35-11.40	222,99	4,00	112,48	52,24%											
	S3-11.75-11.78	57,02	2,25	17,26	34,22%											
S3-B	S3-12.20-12.25	93,38	3,30	32,76	38,62%	A	A	R	C	R	R				R	
	S3-12.50-12.55	94,00	5,15	37,14	44,99%	C	A	R	A	C	C	R			R	
	S3-12.75-12.80	121,68	6,98	50,13	46,93%	C	C	R	C		R				R	
	S3-13.10-13.15	169,04	12,82	77,76	53,58%		C		R							
	S3-13.30-13.35	93,38	1,21	37,78	41,75%		R		R	R						
S3-A	S3-14.70-14.75	116,66	9,32	65,08	63,78%											
	S3-15.80-15.85	99,61	5,23	58,73	64,21%											
	S3-16.85-16.90	194,16	0,76	88,05	45,74%											
	S3-17.15-17.20	139,54	0,81	50,61	36,85%											
	S3-17.96-18.00	103,72	2,50	64,36	64,46%											
	S3-18.90-18.95	165,49	21,13	88,53	66,26%											
	S3-19.35-19.38	98,01	1,00	44,37	46,29%											
	S3-19.85-19.90	125,45	18,29	46,97	52,02%											
	S3-20.55-20.60	109,33	26,78	47,59	68,02%											
	S3-21.10-21.14	53,96	6,62	26,43	61,25%											

Tab. 3 - Results of the macro- and micropaleontological analyses from the S3 borehole. Legend: A = abundant; C = common; R = rare; R? = not in place.

mens.

Moreover, vegetal remains are abundant, including fruits of *Ruppia* (Martinetto, personal communication). The upper part of the borehole, between S2 4.51-4.58 and S2 1.80-1.88 (Interval S2-E in Tab. 2) is characterized by oligotypic assemblages composed of mollusks (only *Cerastoderma glaucum*, *Abra ovata* and *Hydrobia* sp.), ostracods (only non-ornamented taxa) and foraminifers, with rare specimens of *Ammonia tepida* and *Nonion depressulum*. Here abundant vegetal remains (including *Ruppia* fruits and Characeae oogons - only the internal organic lining) are also present. The upper-


1
10 µm
2
10 µm
3
10 µm
4
20 µm
5
10 µm
6
20 µm
7
10 µm
8
10 µm
9
10 µm
10
50 µm
11
10 µm
12
10 µm
13
14
15
16
10 µm

most part of the succession, from sample S2 1.48-1.58 to sample S2 1.18-1.28 (Interval S2-F in Tab. 2), contains only vegetal remains.

S3 Borehole

Fossil remains first occur in sample S3 13.30-13.35 (base of Interval S3-B in Tab. 3) and they are represented by rare vegetal remains and very rare mollusks fragments of *Cerastoderma glaucum* and *Abra ovata* (Tab. 3). From this level up to S3 12.20-12.25 (top of Interval S3-B in Tab. 3), the assemblages are richer, but not diversified. In fact, among the mollusks, only *Hydrobia* genus is added to the species mentioned above. In Interval S3-B, ostracods (with non-ornamented valves) and benthic foraminifers (with rare *Ammonia tepida* and *Nonion depressulum*) first occur; the remains of plants are abundant, and among them *Ruppia* fruits are present.

From sample S3 11.75-11.78 to sample S3 8.65-8.70 (Interval S3-C in Tab. 3), the fossils are rare and represented by vegetal remains found in two levels only. From sample S3 8.40-8.46 to sample S3 1.80-1.85 (Interval S3-D in Tab. 3), the assemblages resemble those of Interval S3-B (Tab. 3), with abundant plant remains (including *Ruppia* fruits), mollusks (*Cerastoderma glaucum*, *Abra ovata* and *Hydrobia* sp.), ostracods (with non-ornamented valves), scarce remains of fishes and insects and also benthic foraminifers, with *Ammonia tepida* and *Nonion depressulum*.

The top of the borehole, from S3 1.50-1.55 to S3 0.93-1.00 (Interval S3-E in Tab. 3), contain very abundant vegetal remains only.

4.3.2. Palynology

Palynological samples provided rich palynomorph assemblages solely for the upper portions of S2 and S3 cores; selected photos of palynomorphs from S2 and S3, at light microscopy, are shown in Figure 8.

S2 borehole

Fourteen samples from S2 were submitted to palynological analyses. The lowest four samples, located between -23.45 and -6.15 m, are barren in palynomorphs. The ten fertile samples, between -5.10 and -1.18 m, consist of sand with clayey silt and dark clay with sandy silt deposits. Their pollen concentration ranges from 681 grains/g (S2 3.33-3.43) to 32,897 grains/g (S2 4.00-4.10). All detected pollen taxa (69) are listed, with the respective percentages for each sample, in the palynological diagram of Figure 9.

Among the arboreal plants (AP, 21 taxa) both de-

<<<<<-- ----------

Fig. 8 - Selected pollen grains from S2 and S3 boreholes. 1 = *Pistacia*; 2 = Cannabaceae; 3 = *Vitis*; 4 = *Ephedra distachya* type; 5 = *Quercus suber* t.; 6 = *Betula*; 7 = *Artemisia*; 8 = *Celtis*; 9 = *Ulmus*; 10 = Poaceae; 11 = *Hedera*; 12 = *Fagus*; 13 = *Abies*; 14 = *Tilia*; 15 = *Cistus*; 16 = *Quercus ilex* t.

---------- -->>>>>

Fig. 9 - Detailed palynological diagram of S2. On the left the samples and the sum of Arboreal and Non-Arboreal Pollen (AP, NAP). *: peak of *Pseudoschizaea*.

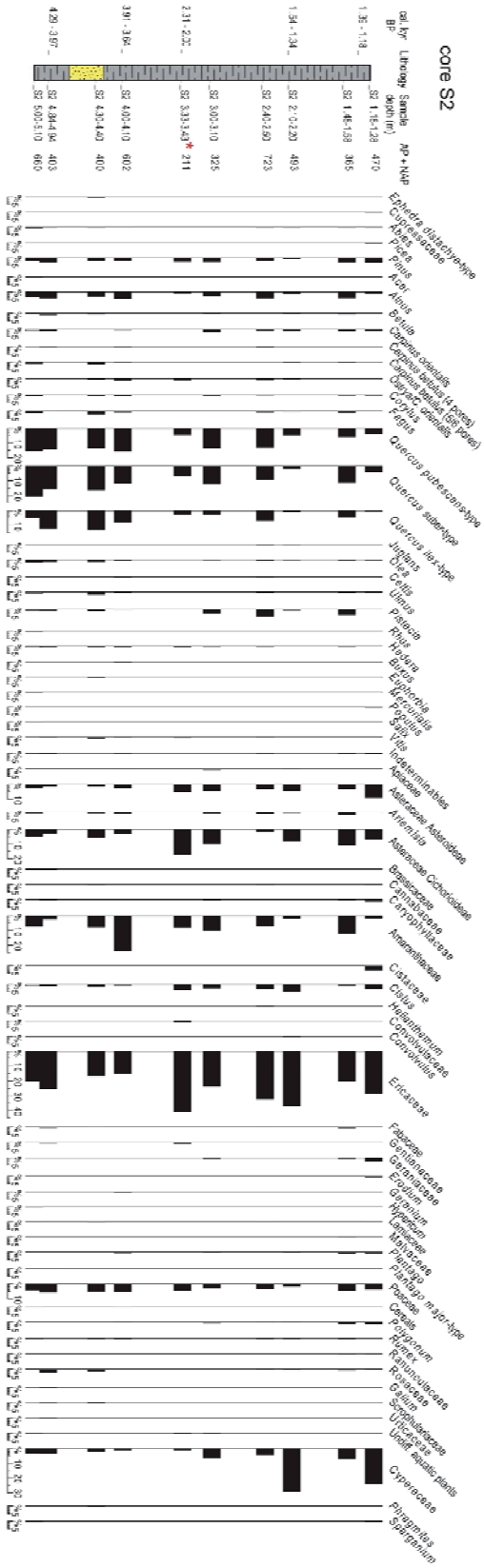

ciduous and evergreen oaks (*Quercus pubescens* type, *Q. suber* type and *Q. ilex* type) reach quite high proportions up to 40%. *Pinus* is continuously present though in low values generally between 1 and 3%. *Alnus* (1.0 to 4.7%) is followed on lower values, by many other arboreal taxa such as *Carpinus* (*C. orientalis* and *C. betulus*), *Fagus*, *Olea*, *Betula*, *Ulmus*, *Corylus*, *Picea*, *Abies*, *Acer*, *Celtis*, *Juglans* and Cupressaceae. 48 Non-Arboreal Plants (NPA) taxa were detected. *Pistacia* reaches good percentage (0.2 to 3.6%). Rare: *Hedera*, *Vitis*, *Rhus*, *Buxus*, *Euphorbia*, *Mercurialis*. Ericacee, often dominant (15 to 37%), are followed by Amaranthaceae (1.5 to 23.8%) and Asteraceae (Cichorioideae and Asteroideae, from 1.0 to 17%). Samples at the core top (from the sample S2 3.00-3.10 to the sample S2 1.18-1.28) showed a good occurrence of Cyperaceae too (up to 30%). Present in good quantity Poaceae (1.6 to 5.7%) and *Cistus* (0.2 to 4.7%). More discontinuous: Apiaceae, *Artemisia*, *Plantago*, Brassicaceae, Cannabaceae, Caryophyllaceae, Cistaceae, *Helianthemum*, Convolvulaceae, *Convolvulus*, Fabaceae, Gentianaceae, Geraniaceae, *Erodium*, *Geranium*, *Hypericum*, Lamiaceae, Malvaceae, Cereals, *Polygonum*, *Rumex*, Ranunculaceae, Rosaceae, *Galium*, Scrofulariaceae, Urticaceae and *Sparganium*. Spores of Pteridophyta (trilete and monolete) are also present. Dinocysts and other algae are present albeit sporadically. Dinocysts were observed in S2 6.15-6.23 (*Polysphaeridium zoharyi*) and S2 4.30-4.40. A peak of *Pseudoschizaea* is recorded in S2 3.33-3.43 sample.

As a summary, with the exception of the three deepest samples, between -5.10 and -4.30 m, for which the arboreal plants percentage is slightly greater than that of herbaceous plants and shrubs, in the above samples is observed a dominance of non-woody plants (up to 80%) which is especially significant for samples S2, 3.33-3.43, 2.00-2.10 and 1.18-1.28. Altitudinal arboreal taxa such as *Abies*, *Betula* and *Fagus* (one pollen grain of *Picea* in S2 1.18-1.28 sample), though always with a few grains, are a constant presence throughout the diagram. Even *Pinus*, always below 3%, does not show significant variations even in correspondence of the major changes in the depositional environment.

Starting from 5 m BGS, the palynological record shows a good occurrence of tree taxa largely represented by deciduous and evergreen oaks with values up to about 40%. The Amaranthaceae expansion highlights the establishment of a salt marsh at -4.00, -4.30 m (over 20% in S2 4.00-4.10). This is followed at -3.33 to -3.43 m by a phase characterized by a good presence of NAP both herbaceous (Asteraceae, *Cistus*, Poaceae) and shrubs (Ericaceae, *Pistacia*), as well as from a minimum in the pollen concentration values and a spike in *Pseudoschizaea*. Upwards increasing NAP is mainly linked to the expansion of Ericaceae, which is sometimes in parallel to that of Cyperaceae (S2: 2.00-2.10 and 1.18-1.28) which marks the establishment of a freshwater environment. To underline two minima in the percent-

---------- -->>>>>

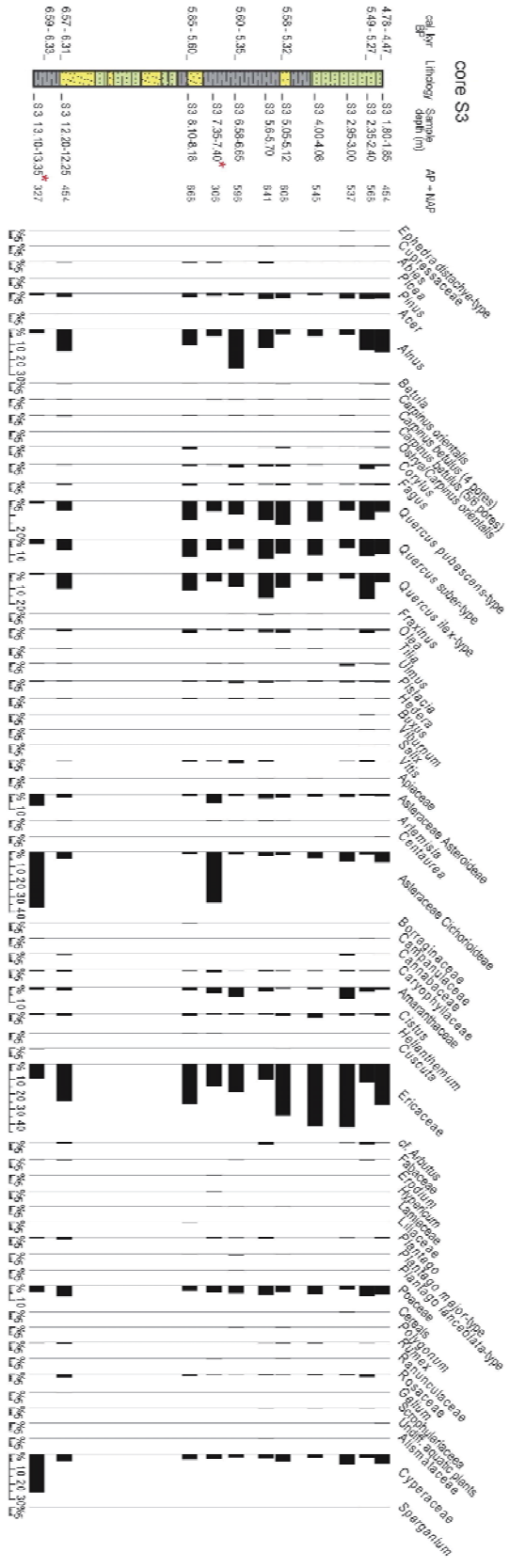

Fig. 10 - Detailed palynological diagram of S3. On the left the samples and the sum of Arboreal and Non-Arboreal pollen (AP, NAP). *: peak of *Pseudoschizaea*.

ages of both deciduous and evergreen oaks in correspondence of the two phases of expansion of Cyperaceae and Ericaceae, in S2 2.00-2.10 and S2 1.18-1.28 samples.

S3 borehole

Fourteen samples from S3 were taken for palynological analyses (Fig. 10), three of them were barren in palynomorphs. All rich palynomorphs samples come from deposits, mainly consisting of clayey silt and dark clays with sandy silt.

The eleven fertile pollen samples exhibit high concentration values, ranging 743 grains/g (S3 7.35-7.40) to 76,684 grains/g (S3 1.80-1.85) (Fig. 10). 62 pollen taxa have been detected. The arboreal plants (AP, 20 taxa) mainly consist of deciduous and evergreen oaks (up to about 40%) and *Alnus* (2.75 to 25.9%). *Pinus* ranges between 1.1 and 3.7%. *Corylus* (up 2.8%), *Olea* (up 2.3%) and *Fagus* (up 1.3%) are present, sometimes in good quantities. Follow *Carpinus* (*C. orientalis* and *C. betulus*), Cupressaceae, *Abies*, *Picea*, *Acer*, *Betula*, *Fraxinus*, *Tilia* and *Ulmus*. Non-arboreal plants (NAP, 42 taxa) are represented by shrubs like *Pistacia* (up 1.5%), *Hedera*, *Buxus*, *Viburnum* e *Vitis*. Ericacee range between 9.5 and 42%. Among the herbaceous taxa are present Asteraceae Cichorioideae (1.5 to 37.3%), Cyperaceae (2.3 to 25.7%), Poaceae (2.8÷7.5%) and Amaranthaceae (0.6÷7.6%) followed by Asteraceae Asteroideae (0.8÷7.3%) and *Cistus* (0.2 to 2.7%). More sporadic: Apiaceae, *Artemisia*, *Centaurea*, Borraginaceae, Campanulaceae, Cannabaceae, Caryophyllaceae, *Helianthemum*, *Cuscuta*, cf. *Arbutus*, Fabaceae, *Erodium*, *Hypericum*, Lamiaceae, *Plantago* (*P. mayor* t. and *P. lanceolata* t.), cereals, *Polygonum*, *Rumex*, Ranunculaceae, Scrofulariaceae, Rosaceae, *Galium*, Alismataceae, Liliaceae and *Sparganium*. Spores of Pteridophyta (trilete and monolete) and algae are also present. Dinocysts occur in all samples excepted in S3 5.05 -5.12; *Pseudoschizaea*, never absent, shows a main peak at S3 7.35-7.40 and a secondary one at S3 13.10-13.15.

The palynological record begins at -13.10 m with a phase dominated by the non-arboreal plants in coincidence with a minimum in the concentration values and a good occurrence of *Pseudoschizaea*. Among the NAP prevail Asteraceae Cichorioideae followed by Cyperaceae, Ericaceae, A. Asteroideae and Poaceae. Cyperacee, in particular, recorded here their main peak of abundance, reaching 26%. Trees showed a subsequent increase at 12.20-12.25 m, attested by the presence of several species of *Quercus* and *Alnus*, which are followed by *Pinus* and *Olea*. *Carpinus* (*C. betulus* and *C. orientalis*), *Corylus*, *Acer*, *Tilia* and *Ulmus* are also present. Among the altitudinal arboreal taxa, although always low, there are *Abies*, *Fagus* and *Betula*. Among the NAP to remark the abrupt fall of A. Cichorioideae (from 37.3% to 4.6%) and the sharp increase of Ericaceae from 9.5% to 24.5%.

The palynological record, after the barren interval linked to the occurrence of unfavorable sediments for pollen preservation, starts again from -8.10 m. From here up to -1.80 m is observed a dominance, albeit marked by successive fluctuations between arboreal (oaks with peaks in S3: 8.10- 8.18; 5.60-5.70; 5.05-5.12; 4.00-4.08; 2.35-2.40) and non-arboreal plants (Ericaceae). Ericaceae record a maximum (42%) in 2.95 -3.00 m in correspondence to a phase of decline of the oaks: *Q. ilex* in particular presents here its second minimum value (3.35%), after that characterizing the base of the succession (0.61%). The Cyperacee, though still present, are reduced to values ranging between 2.3% and 7%. At -7.30 m a minimum in the pollen concentration values falls in coincidence, again, with a main peak of *Pseudoschizaea*. Moreover this level is characterized by a sharp increase in Asteraceae, especially Cichorioideae, reaching 34% and by a phase of temporary reduction of *Alnus,* oaks and Ericaceae.

In all S3 samples, *Pinus* and *Olea*, although always present, are never abundant. The same pattern was also observed in S2.

5. DISCUSSION

5.1. Sedimentary architecture and depositional settings

The collected data permitted to detect four main depositional environments and associated facies (Figs. 5, 11, 12).

1) Fluvial (F)

It has been observed throughout S1 and S4, in the lower half of S2, and in the lower and middle portion of S3. It is mainly expressed by an alternation of gravels and sands/silts weakly clayey (SU 1a and SU 1b in S1, S2, S3); an alternation of silty clayey sands and silts with sandy clay (SU 1c in S3); a succession largely consisting of clayey sandy silts, with intercalated, silty-clayey or sandy-silty gravels beds (SU 1d in S4). Gravels, from matrix support to open work texture, are heterometric, heterogeneous and subangular. Gravels sometimes show an inverse gradation; the finer ones are sometimes characterized by yellow-brown mottles and thin sandy plane-parallel laminae with oxidation from ocher to reddish color. Alluvial plain deposits depict the occurrence of channel and floodplain facies, with intercalated debris flows. Samples are generally barren in both palynomorphs and marine/brackish fossils (Interval S2-A, S2-C, S3-A, S3-C).

2) Marine (M)

A marine depositional environment is only detected in the medium-upper portion of S2 where it rests on fluvial deposits by a sharp and erosive contact. It includes two main facies (M1 and M2).

- M1-Shallow marine. The facies, about up to 80 cm thick (from 11.90 to 11.10 m BGS), consists of fine, silty and clayey sands with abundant fragments of mollusks shells (SU 2a). It attests a short-term episode interrupted by the instauration of a fluvial environment, expressed by gravelly deposits (SU 1a). The fossil assemblage suggests a very shallow water, probably referable to a submerged beach environment (interval S2-B).
- M2-Marine infralittoral. Rich microfossil assemblages were recovered throughout the S2 succession, from

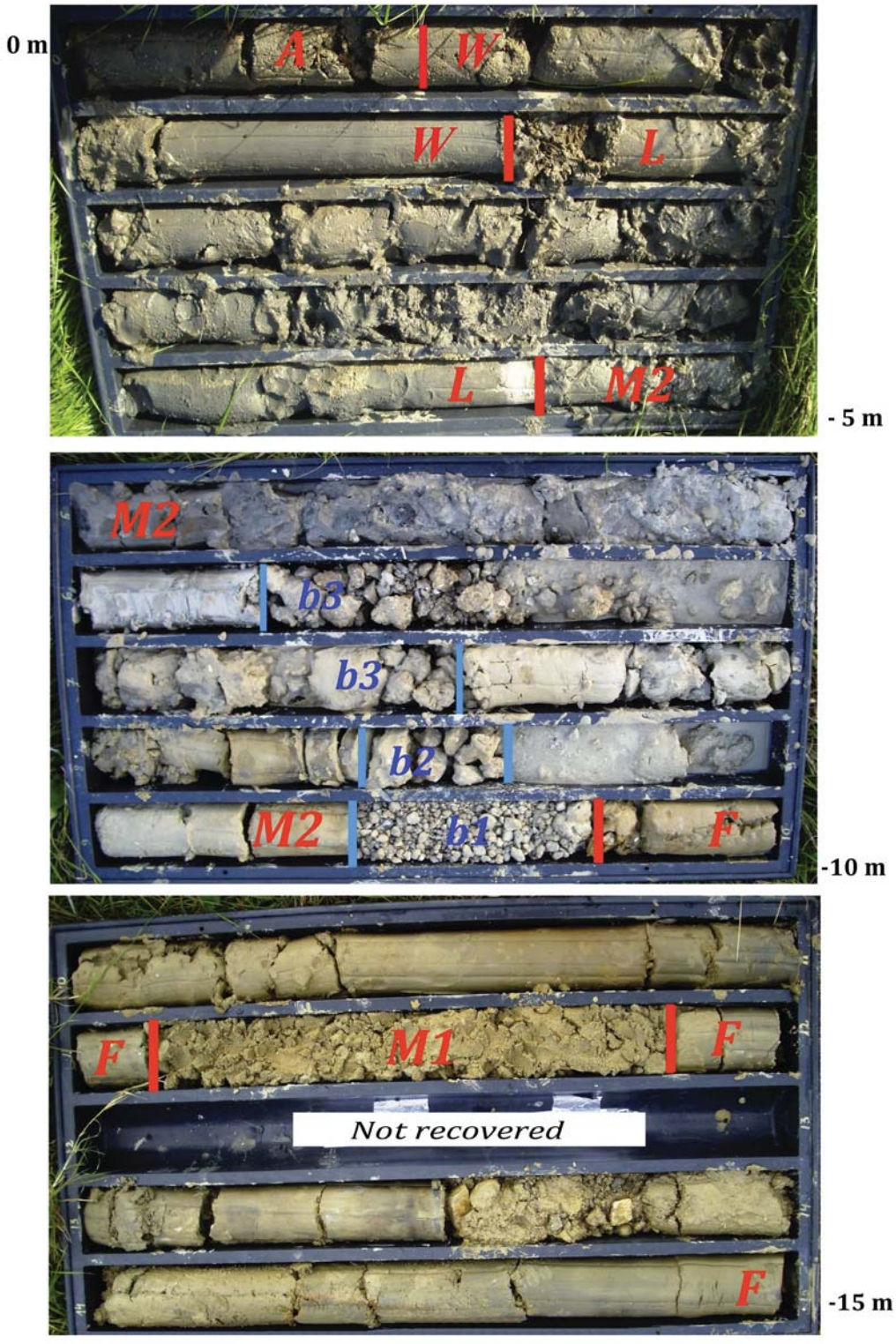

Fig. 11 - Classification boxes containing core samples (between 15,00 and 0,00 m BGS) from S2 borehole. Legend: F = fluvial deposits; M1 = shallow marine deposits; M2 = marine infralittoral deposits (b1-b3 = biocalcarenite strata); L = brackish lagoon deposits; W = fresh-water wetland deposits; A = anthropogenic terrains.

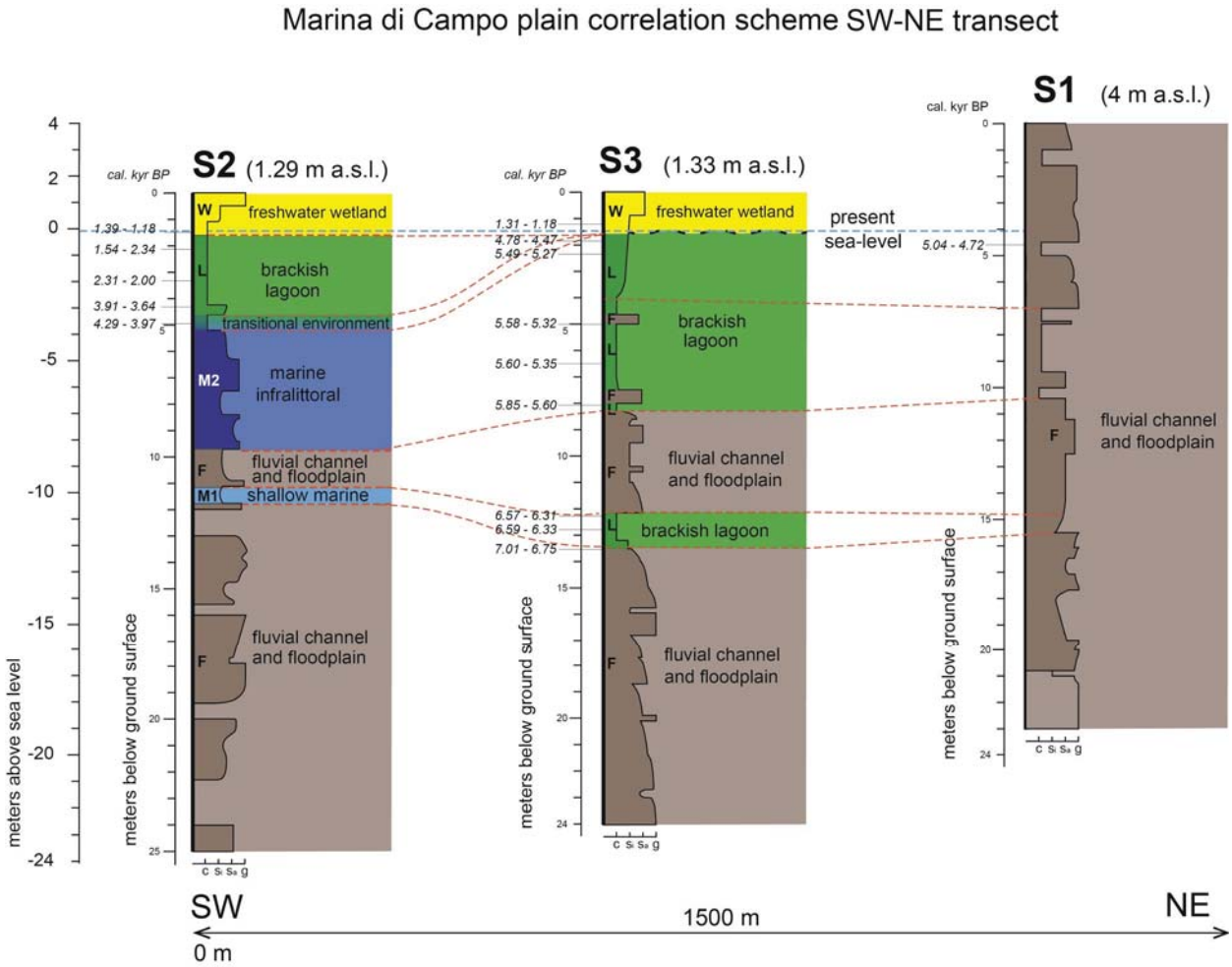

Fig 12 - SW-NE transect at Marina di Campo plain: paleoenvironmental reconstruction and attempt of correlation between S2, S3 and S1 sedimentary cores.

9.70 to 4.60 m BGS. It consists of sands, silty-clay sands, sand with silty clays and clays with sandy silts which alternate with three biocalcarenite levels: the first one between 9.70 and 9.40 m, the second one between 8.50 and 8.40 m and the third one between 7.50 and 6.30 m BGS (SU 2b and lower part of SU 3). The higher diversified microfossil assemblages, especially benthonic foraminifers (among the most common: *Ammonia beccarii*, *Asterigerinata mamilla, Elphidium* spp. and *Quinqueloculina* spp.) as well as the presence of rare planktonics in all the sample of the interval, attest the instauration of more open marine conditions than the previous interval (M1) and possibly of slightly deeper waters starting from 9.30-9.40 m BGS, referred to infralittoral environment (Interval S2-D).

It is interesting to note that, anyway, from S2 5.30-5.40 m (SU 3), significant changes in the assemblages are marked by the appearance, among mollusks, of the genera *Cerastoderma*, *Abra* and *Hydrobia* and among ostracods, of a large number of non-ornamented specimens. Vegetal remains are abundant, including fruits of *Ruppia*.

3) Brackish lagoon (L)

The upper portions of both S2 (from 4.60 to 1.60 m BGS) and S3 (from 13.50 to 12.15 and from 8.30 to 1.60 m BGS) consist of organic clay with sandy silt, dark gray in color and very plastic (SU 3), associated to a brackish lagoon environment (backdune) as registered by microfossil assemblages. In S2 the passage from marine (M2) to lagoon environment seems to occur gradually, in continuity of sedimentation.

In S3 microfossil assemblages, though rather oligotypic and monotonous support the instauration of a predominantly brackish lagoon environment (Intervals S3-B and S3-D). The latter, however, was affected by three alluvial events promoting an increase of the detrital input and the sedimentation of three coarser strata from about 50 cm to 385 cm thick (SU 1c).

In S2 microfossil assemblages depict a predominantly brackish lagoon environment for a total 2.80 m thickness (Interval S2-E), with two short phases of increase of detrital input between 4.35 and 4.65 m and between 3.30 and 3.45 m BGS (SU 1c). Values up to 24% for Amaranthaceae attest the larger expansion of the saltmarsh at ~4 m in S2.

The repeated interruptions of the lagoon sedimentation matched *Pseudoschizaea* peaks and strong reduction in the concentration values of palynomorphs. This evidence supports an increase of the erosive processes in the surrounding reliefs, during a phase of reduction of the vegetation cover, with a consequent increase in river sedimentation rates in a brackish lagoon subjected, however, to seasonal drying.

4) Freshwater wetlands (W)

Silt with weakly sandy clay in the topmost portion of both S2 (from 1.60 to 0.50 m BGS) and S3 (from 1.60 to 0.87 m BGS) (SU 3) contains only very rare Characeae and other abundant vegetal remains typical of freshwater coastal ponds (Intervals S2-F and S3-E). Cyperaceae values up to 29% in S2 (at 2.10 m BGS) attest the extension of freshwater wetlands.

5.2. Main environmental changes on southern Elba Island during the late Quaternary

Climate and sea level changes played an important role on late Quaternary aquatic and terrestrial environments in the central Mediterranean (e.g. Benjamin et al., 2017; Vacchi et al., 2017; 2018; Antonioli et al., 2018; Sadori, 2018 and references therein).

The stratigraphic framework reconstructed for the subsurface of Marina di Campo area shows remarkable similarities with those from several coeval late Quaternary successions in the Mediterranean area (see Amorosi & Milli, 2001 and reference therein). In fact, in spite of modest differences at local level, in the Mediterranean coastal areas the sedimentary history of the last 125 kyrs is characterized by a series of transgressive-regressive deposits, generally represented, starting from the oldest ones, by: i) marine sediments of the last interglacial (MIS 5.5, Highstand System Tract - HST); ii) alluvial deposits of the last glaciation (MIS 4-2, Lowstand System Tract - LST); iii) transgressive and highstand post-glacial alluvial, coastal and marine deposits (Trasgressive System Tract - TST and Highstand System Tract - HST) (Zaitlin et al., 1994).

At EI, the latest Pleistocene phases did not leave evident and continuous sedimentary evidence. This is the case of the Tyrrhenian transgression during MIS 5.5 which is indeed well attested by marine sediments and platforms along the Tuscan peninsular coast and in the neighboring island of Pianosa (Graciotti et al., 2004; Antonioli et al., 2011). In the Marina di Campo hinterlands as well as in the other coastal plains of Elba, fluvial terraces, between 10 and 15 m above sea level, suggest a higher base level than the current one, i.e. a sea level highstand of MIS 5.5 (D'Orefice & Graciotti, 2018).

The regressive phases during MIS 4 and MIS 2 promoted the emersion of the Tuscan continental platform including the area in front of Marina di Campo. Sea level was significantly lower (LST) compared to today, of about 80÷90 m during MIS 4 and even around 120 m during MIS 2 (Waelbroeck, 2002; Peltier & Fairbanks, 2006; Lambeck et al., 2011). However, during MIS 3 (Zecchini, 1981), EI returned, after the previous dominant continental phase during MIS 4, to be isolated from the Italian peninsula as during the Tyrrhenian (MIS 5.5).

During MIS 2 (including the LGM) the Tuscan continental platform, almost completely emerged, was deeply incised by a hydrographic network (Bianchi, 1943; Bartolini et al., 1979), which deepened progressively landward because of upstream knickpoint migration. The incised valleys formed during the phases of relative sea level fall have been widely described in the literature (Zaitlin et al., 1994), with particular reference to the late Pleistocene glacials (e.g. Suter & Berryhill, 1985; Posamentier & Allen, 1999). Subsequently, in these wide and deep valleys, predominantly fluvial coarse sediments, many meters thick, were deposited as attested in the subsoil of the Marina di Campo plain by the lower portion of S1-S4. This is also confirmed by numerous boreholes, reported in Bencini et al. (1986), that reached the bedrock at depths even greater than 40 m near the present coastline (see also D'Orefice & Graciotti, 2018). The considerable availability of sediment from river systems possibly related to the overall decrease in the vegetation cover during prevalent dry conditions. Short and intense precipitation events were, in their turn, responsible for a large part of the total sediment transport. The absence of datings does not allow to frame these river deposits in a precise chronological interval. However, according to other regional contributions (e.g. Amorosi et al., 2003, 2004; Aguzzi et al., 2007; Milli et al., 2016) it is conceivable to attribute this sedimentary episode to the late phase of low standing (Late Lowstand System Tract - LLST) of the late Pleistocene.

Between the end of the Pleistocene and the beginning of the Holocene sea level rose very quickly (an average rate of rise of 15 m/kyr, Lambeck et al., 2002, 2014), leading to a rapid retreat of the coastline. In this context, the transgressive deposits (TST), characterized by marine (S2) and lagoon sediments (S3), mainly including fine sands, sandy silts and clays, overlie with a sharp erosional boundary the alluvial gravels and sands. The erosional boundary and the abrupt facies change, suggest the presence of a significant stratigraphic hiatus due to a prolonged erosive phase. This erosional boundary most likely represents the continuation of the late Pleistocene erosive surface, identified by geophysical surveys, in the EI offshore (Principi et al., 2015b). A similar erosional surface has also been identified in other Italian coastal areas; for example in the upper Adriatic (Amorosi et al., 1999; 2003; 2004 and references therein) or in the lower plains of the Arno (Aguzzi et al., 2005; 2007; Amorosi et al., 2008; 2009), where, probably, it is associated to a stratigraphic hiatus including the Late Glacial and part of the Holocene.

During the early phase of the Holocene transgression, in the Marina di Campo area the sea penetrated inside the pre-existing fluvial valleys, as documented at S2, i.e. the closest site to the current coastline compared to S3, S1 and S4. The last two cores, in fact, include only alluvial deposits (Fig. 5) being located in a much more internal position with respect to both S2 and S3. In the study area, the first marine evidence can be placed around 7,000 cal. yr BP on the basis of the AMS datings (Tab. 1) of the dark organic lagoon silts and clays in S3 (about 135 cm thick between 13.50 and 12.15 m bgs). This level probably correlates with the first evidence of marine deposits (M1, Figs. 11, 12), between

11.90 and 11.10 m BGS in S2. Indeed, lagoon deposits at S3 possibly represent the lateral landwards equivalent of S2 marine deposits (Fig. 12).

Holocene fine lagoon deposits, characteristic of a low-energy environment, as before mentioned, overlap the coarser late Pleistocene alluvial sediments, attesting a sudden sedimentary environment change at S3. They accumulated inside shallow brackish basins, delimited towards the sea by coastal barriers progressively migrating landward during the phase of post-glacial transgressive sea level rise. The absence of marine deposits in S3 can be justified by its position slightly further from the current coastline than S2. This position, during the Holocene transgression, could be even more internal due to a different conformation of the coastline, which probably was more advanced in its northern section than the southern one. The hypothesis now formulated is supported by the presence, behind the northern coast, of a much larger catchment basin. It would have ensured, through its hydrographic network, a greater sediment contribution from the hinterland, determining the more advanced position of the northern coastal sector than the southern one.

Within the Holocene transgressive succession, however, there is a brief regressive episode, attested by fluvial deposits (mainly sandy and silty) in both S2 (between 11.10 and 9.70 m BGS) and S3 (between 12.15 and 8.30 m BGS), which interrupt, respectively, the marine and lagoon sedimentation (Fig. 12). This episode can be attributed to a minor oscillation of the sea level, possibly due to a relatively small climate changes (Pascucci et al., 2018), between ca 6,600 and 5,800 cal. yr BP in S3.

The final phases of the Holocene transgression (ca 6,000 cal. yr BP) are marked by a second frankly marine episode (M2). Slightly deeper waters, in an infralittoral environment, can be reconstructed starting from 9.30-9.40 m BGS in S2, especially by fossiliferous sands and silts, interbedded to three biocalcarenite layers.

Starting from about 6,000 cal. yr BP, the eustatic rise became slower (less than 1 mm/yr), as also recorded throughout the Mediterranean (Anthony et al., 2014; Vacchi et al., 2016; Ghilardi et al., 2018; Melis et al., 2018), and the highstand sea level (HST) began. During this phase, the sediment input from the hinterland took over the creation of sedimentary space; thus, the progradation towards the sea of coastal and river systems began, with consequent depositional regression of the coastline. In S2 this corresponds to a change in faunistic assemblages attesting a decrease of the sea waters depth and a gradual upwards shift, between 5.40 and 4.60 m BGS, to a full brackish lagoon environment. Indeed, above this gradual passage, between 4.60 and 1.60 m BGS, the conditions for the development of permanent lagoons in the areas behind a prograding Holocene coastal barrier established near the coast. The most recent evidence of the coastal barrier, consisting of beach and dune ridges, is in external position, in correspondence of the present coastline (Fig. 4).

In the most internal areas, the HST is expressed, from about 8.00 m BGS in S3, by predominantly clayey sediments which deposited in a lagoon environment. In S1 a decrease in the mechanical energy is attested in fluvial deposits by the reduction in the size of the granulometric fraction, represented by weakly sandy silty clays, between 10.40 and 7.00 m BGS (Fig. 5). This level corresponds to lagoon deposits in S3 (Fig. 12).

In S3 and S2 the lagoon sedimentation ends at 1.60 m BGS, but while in the inland areas (S3) it ends shortly after 4,780 – 4,470 cal. yr BP, in the coastal areas (S2) the lagoon sedimentation persisted until about 1.60 m BGS, at about 1,500-1,400 cal. yr BP (Fig. 6). During both TST and HST, the sedimentation in the lagoon was rather discontinuous being affected by frequent interruptions, corresponding to episodes of increase in both solid input and coarser granulometric fraction. Lagoons were in fact submitted to seasonal drying after high-energy alluvial events as also attested in the palynological record (*Pseudoschizaea* peaks and decrease of palynomorphs concentration).

With the definitive closure of the communication with the open sea, attested by the gradual disappearance of the brackish faunas, the lagoons at Marina di Campo were progressively transformed into freshwater coastal ponds between the end of Roman times (at about 1,500 cal. yr BP) and the Early Middle Ages (<ca 1,300–1,200 cal. yr BP). In these low energy depositional environments silts and dark clays accumulated; abundant plant remains (S2 and S3) were also found. In the areas bordering the ancient coastal ponds, fluvial sedimentation persisted up today conditioning the development of the current alluvial plain. The prevalent sandy and silty fluvial sediments covering to some extent the lagoon and freshwater wetlands ones reducing their areas of outcrop.

The pilot palynological approach developed in the frame of the geomorphological map survey, despite still lacking adequate resolution, especially for paleoclimate reconstructions, made possible to furnish some additional and complementary evidence on the depositional environments. Investigation in S2 and S3 provides, specifically, some paleovegetational and paleoclimatic spots in the interval extending from the upper portion of the Neolithic up to the Early Middle Ages which largely center the period characterized by increasing aridification phenomena (Mayewski et al., 2004; Jalut et al., 2009; Roberts et al., 2011; Bini et al., 2019). From about 6,000 years BP repeated phases of enlargement and narrowing of the forest vegetal formations are well evident in both Marina del Campo records, at S2 and S3 (Figs 9, 10). The most recent decrease in tree cover at S2, seems connected to the early stages of increasing human activities related to metallurgy (Etruscan civilization). Magnetic susceptibility studies in marine cores taken from the area between the Elba and Corsica Islands (Vigliotti et al., 2003), documented, in fact, an important metallurgical activity during this time with a maximum peak localized around 2,500 years BP. Instead, the low abundance of cultivated taxa (e.g. cereals, *Vitis*, *Juglans* and *Castanea*) leads to the exclusion of intense agricultural exploitation of the area. It is clear that higher resolution palynological analyses, now in progress, are indispensable to document the successive phases of increase / drastic reduction of oak trees (both deciduous and evergreen) or rather of Non-Arboreal Plants, as well as changes in the extension of coastal

wetlands, characterized by the expansion of marsh or swamps. The occurrence of salt (e.g. as attested by the increase of Amaranthaceae in S2 at 4-4.1 m) and/or freshwater (as attested by the increase of Cyperaceae at the base of S3 or at the upper portion of S2 and/or *Alnus*) wetlands is also well documented during the lagoon phase development. The new ongoing studies on EI cores, integrated by those from the main Italian sites, already known in bibliography (e.g. Currás et al., 2017; Di Rita et al., 2018 and references therein; Melis et al., 2018; Sadori, 2018), possibly, will lead to a more coherent interpretation and reconstruction of the role played by climate and / or man during this crucial time at the Middle-Late Holocene transition in the central Mediterranean area.

CONCLUSIONS

The multidisciplinary study of 4 continuous core drillings (S1÷S4) provided the unique opportunity, in absence of sedimentary outcrops, to document the late Quaternary sedimentary succession of southern EI. Noteworthy, the presence of Holocene marine deposits in the subsoil of EI is attested, for the first time.

Three main depositional phases representing the paleoenvironment response to the glacial-eustatic sea level rise starting from LGM, i.e. 1. low stationing phase (Lowstand Systems Tract - LST), 2. transgressive phase (Transgressive Systems Tract - TST); 3. high stationing phase (Highstand Systems Tract - HST) have been described.

LST - During the LGM lowstand the continental shelf facing the Marina di Campo area was completely emerged and strongly carved by the hydrographic network. As a result several tens of meters of coarse river sediments accumulated in these valleys, during the latest Pleistocene.

TST - During the transgressive post-glacial phase, between the end of the Pleistocene and the beginning of the Holocene, the sea level rising promoted a progressive withdrawal of the coastline, the deactivation of river sedimentation and the migration towards the land of a barrier-lagoon system. In this context, around 7,000 cal. yr BP, in the easternmost sector of the Marina di Campo plain (which extends from the current coastline up to about 400-500 m landwards) a marine shallow water environment developed. Brackish lagoon expanded in the innermost coastal sector, while fluvial environments developed in the upper zones. After a brief regressive episode, between ca 6,600 and 5,800 cal. yr BP, attested by fluvial deposits which interrupt the marine and lagoon sedimentation, a slightly deeper marine environment established in the easternmost sector. In the innermost zones, however, the lagoon sedimentation continues, with some interruptions due to the increase of solid input in the lagoon basins, following high-energy alluvial events. Lagoons were in fact submitted to seasonal drying following high-energy alluvial events as also attested in the palynological record (*Pseudoschizaea* peaks and decrease of palynomorphs concentration).

HST - Around 6,000 cal. yr BP, the sediment input from the hinterland takes over the creation of sedimentary space, after the transgressive phase and the start of the highstand sea level. The progradation towards the sea of coastal and river systems begins, with consequent depositional regression of the coastline; brackish lagoon sedimentation extends to the eastern sector before being interrupted by alluvial episodes. Between about 1,500 cal. yr BP and approximately 1,300–1,200 cal. yr BP, with the definitive closure of the communication with the open sea, the lagoon areas at Marina di Campo were progressively transformed into freshwater coastal ponds. In the surroundings of the ancient coastal ponds, fluvial sedimentation persists until today as attested by the current floodplain.

This contribution provides a geological-stratigraphic basis for future research on relevant topics and questions still open concerning especially the:

i) stratigraphic relationships and chronology of fluviatile and marine deposits which exhibit a sharp erosive contact. At present the occurrence of unreliable AMS datings of marine sediments and the absence of chronological references in fluvial sediments prevent any inferences;

ii) reconstruction of landscape modifications induced by humans and/or climate during the last 7,000 years in the Mediterranean area, including the documentation of the 4.2 kyr event. Multidisciplinary and higher resolution investigations, especially palynological ones, are currently underway at Marina di Campo and in the plains of Magazzini and San Giovanni (central-northern EI).

ACKNOWLEDGES

This study was supported by the ISPRA-Geological Survey of Italy CARG Project, Fondi di Ateneo 2010-12 (University of Florence, Italy) assigned to A. Bertini and Fondi di Ateneo 2010-12 (University of Siena, Italy) assigned to L. Foresi. The authors thank the two anonymous reviewers and Paolo Mozzi (associated Editor at AMQ) for their careful reading of manuscript and for their helpful comments and suggestions.

REFERENCES

AGI - Associazione Geotecnica Italiana (1977) - Raccomandazioni sulla programmazione ed esecuzione delle indagini geognostiche. Edizioni Scientifiche Italiane, Napoli.

Aguzzi M., Amorosi A., Sarti G. (2005) - Stratigraphic architecture of Late Quaternary deposits in the Lower Arno Plain (Tuscany, Italy). Geologica Romana, 38, 1-10.

Aguzzi M., Amorosi A., Colalongo M.L., Ricci Lucchi M., Rossi V., Sarti G., Vaiani S.C. (2007) - Late Quaternary climatic evolution of the Arno coastal plain (Western Tuscany, Italy) from subsurface data. Sed. Geol., 202, 211-229.

Amorosi A., Milli S. (2001) - Late Quaternary depositional architecture of Po and Tevere river deltas (Italy) and worldwide comparison with coeval deltaic successions. Sed. Geol., 144, 357-375.

Amorosi A., Colalongo M.L., Pasini G., Preti D. (1999) - Sedimentary response to late Quaternary sea-level changes in the Romagna coastal plain (northern Italy). Sedimentology, 46, 99-121.

Amorosi A., Centineo M.C., Colalongo M.L., Pasini G., Sarti G., Vaiani S.C. (2003) - Facies architecture and Latest Pleistocene-Holocene depositional history of the Po Delta (Comacchio area), Italy. J. Geol., 111, 39-56.

Amorosi A., Colalongo M.L., Fiorini F., Fusco F., Pasini G., Vaiani S.C., Sarti G. (2004) - Palaeogeographic and palaeoclimatic evolution of the Po Plain from 150-ky core records. Global Planet. Change, 40, 55-78.

Amorosi A., Sarti G., Rossi V., Fontana V. (2008) - Anatomy and sequence stratigraphy of the late Quaternary Arno valley fill (Tuscany, Italy). GeoActa, Special Publication 1, 117-129.

Amorosi A., Ricci Lucchi M., Rossi V., Sarti G. (2009) - Climate change signature of small-scale parasequences from Lateglacial–Holocene transgressive deposits of the Arno valley fill. Palaeogeography, Palaeoclimatology, Palaeoecology, 273, 142-152.

Amorosi A., Bini M., Fabiani F., Giacomelli S., Pappalardo M., Ribecai C., Ribolini A., Rossi V., Sammartino I., Sarti, G. (2012) - MAPPA cores: An interdisciplinary approach. MapPapers 4en-II, 149-200. https://www.mappaproject.org/report-di-progetto/?lang=en

Amorosi A., Bini M., Giacomelli S., Pappalardo M., Ribecai C., Rossi V., Sammartino I., Sarti G. (2013) - Middle to late Holocene environmental evolution of the Pisa coastal plain (Tuscany, Italy) and early human settlements. Quaternary International, 303, 93-106.

Anthony E.J., Marriner N., Morhange C. (2014) - Human influence and the changing geomorphology of Mediterranean deltas and coasts over the last 6000 years: from progradation to destruction phase? Earth Sci. Rev., 139, 336-361.

Antonioli F., Amorosi A.M., Correggiari A., Doglioni C., Fontana A., Fontolan G., Furlani S. Ruggieri Spada G. (2009a) - Relative sea-level rises and asymmetric subsidence in the northern Adriatic. Rendiconti Online Soc. Geol., 34-36.

Antonioli F., Ferranti L., Fontana A., Amorosi A.M., Bondesan A., Braitenberg C., Dutton A., Fontolan G., Furlani S., Lambeck K., Mastronuzzi G., Monaco C., Spada G., Stocchi P. (2009b) - Holocene relative sea-level changes and vertical movements along the Italian coastline. Quaternary International, 221, 37-51.

Antonioli F., D'Orefice M., Ducci S., Firmati M., Foresi L.M., Graciotti R., Perazzi P., Pantaloni M., Principe C. (2011) - Palaeogeographic reconstruction of northern Tyrrhenian coast using archaeological and geomorphological markers at Pianosa island (Italy). Quaternary International, 232, 31-44.

Antonioli F., Ferranti L., Stocchi P., Deiana G., Lo Presti V., Furlani S., Marino C., Orru P., Scicchitano G., Trainito E., Anzidei M., Bonamini M., Sansò P., Mastronuzzi G. (2018) - Morphometry and elevation of the last interglacial tidal notches in tectonically stable coasts of the Mediterranean Sea. Earth-Science Reviews, 185, 600-623.

Bartolini C., Fanucci F., Gabbani G., Rossi S., Valleri G., Lenaz R. (1979) - Studio della piattaforma continentale medio-tirrenica per la ricerca di sabbie metallifere: 2) dall'Isola d'Elba a Livorno. Boll. Soc. Geol. It., 98, 327-352.

Bellotti P., Calderoni G., Dall'Aglio P.L., D'Amico C., Davoli L., Di Bella L., D'Orefice M., Esu D., Ferrari K. Bandini Mazzanti M., Mercuri A.M., Tarragoni C., Torri P. (2016) - Middle-to late Holocene environmental changes in the Garigliano delta plain (Central Italy): which landscape witnessed the development of the Minturnae Roman colony? The Holocene, 26 (9), 1457-147.

Bencini A., Giardi M., Pranzini G., Tacconi B.M. (1986) - Le risorse idriche dell'Isola d'Elba. Quaderni sull'assetto del territorio della Provincia di Livorno, nuova serie, 2, 91, Tacchi Editore, Pisa.

Benjamin J., Rovere A., Fontana A., Furlani S., Vacchi M., Inglis R.H., Galili E., Antonioli F., Sivan D., Miko S., Mourtzas N., Felja I., Meredith-Williams M., Goodman-Tchernov B., Kolaiti E., Anzidei M., Gehrels R. (2017) - Late Quaternary sea-level changes and early human societies in the central and eastern Mediterranean Basin: An interdisciplinary review. Quaternary International, 449, 29-57.

Bini M., Brückner H., Chelli A., Pappalardo M. (2010) - First remarks on the late Holocene relative sea level from sedimentological palaeo sea level indicators in the lower Magra Valley coastal plain. Rendiconti Online Società Geologica Italiana, 11 (1), 34-35.

Bini M., Pappalardo M., Rossi V., Noti V., Amorosi A., Sarti G. (2018) - Deciphering the effects of human activity on urban areas through morphostratigraphic analysis: The case of Pisa, Northwest Italy. Geoarchaeology, 33(1), 43-51.

Bini M., Zanchetta G., Perşoiu A., Cartier R., Català A., Cacho I., Dean J.R., Di Rita F., Drysdale R.N., Finnè M., Isola I., Jalali B., Lirer F., Magri D., Masi A., Marks L., Mercuri A.M., Peyron O., Sadori L., Sicre M.-A., Welc F., Zielhofer C., Brisset E. (2019) - The 4.2 ka BP Event in the Mediterranean region: an overview. Clim. Past, 15, 555-577.

Bianchi E. (1943) - Alcuni effetti delle oscillazioni eustatiche del livello marino sulla morfologia dell'Elba Orientale. Atti Soc. Tosc. Sc. Nat. Mem. Pisa, 52 (2), 23-36.

Blum M.D., Törnqvist T.E. (2000) - Fluvial responses to climate and sea-level change: a review and look forward. Sedimentology, 47(Suppl. 1), 2-48.

Bortolotti V., Pandeli E., Principi G. (con il contributo di D'Orefice M. & Graciotti R.) (2015) - Note illustrative della Carta geologica dell'Isola d'Elba scala 1:25.000. DREAm. Italia.

Boyer J., Duvail C., Le Strat P., Gensous B., Tesson M. (2005) - High resolution stratigraphy and evolution of the Rhône delta plain during postglacial time, from subsurface drilling data bank. Mar. Geol., 222 -223, 267-298.

Bronk Ramsey C. (2008) - Deposition models for chronological records. Quaternary Science Reviews, (1-2), 42-60.

Bronk Ramsey C. (2009) - Bayesian analysis of radiocarbon dates. Radiocarbon, 51, 337-360.

Bronk Ramsey C., Lee S. (2013). Recent and Planned Developments of the Program OxCal. *Radiocarbon, 55* (2-3), 720-730.

Brückner H., Vött A., Schriever A., Handl M. (2005) - Holocene delta progradation in the eastern Mediterranean - case studies in their historical context. Mediterranée. 104, 95-106.

Clark P.U., Dyke A.S., Shakun J.D., Carlson A.E., Clark J., Wohlfarth B., Mitrovica J.X., Hostetler S.W., McCabe A.M. (2009) - The Last Glacial Maximum. Science, 325, 710-714.

Currás A., Ghilardi M., Peche-Quilichini K., Fagel N., Vacchi M., Delanghe D., Dussouillez P., Vella C., Bontempi J.M., Ottaviani J.C. (2017) - Reconstructing past landscapes of the eastern plain of Corsica (NW Mediterranean) during the last 6000 years based on molluscan, sedimentological and palynological analyses. Journal of Archaeological Science: Reports, 12, 755-769.

Di Rita F., Fletcher W.J. Aranbarri J., Margaritelli G., Lirer F., Magri D. (2018) - Holocene forest dynamics in central and western Mediterranean: periodicity, spatio-temporal patterns and climate influence. Scientific Reports, 8(1), n. 8929.

Dini A., Innocenti F., Rocchi S., Tonarini S., Westerman D.S. (2002) - The magmatic evolution of the late Miocene laccolith-pluton-dyke granitic complex of Elba Island, Italy. Geol. Mag., 139, 257-279.

D'Orefice M., Graciotti R. (2008) - Aspetti geomorfologici e sedimentologici dei depositi eolici del settore occidentale del promontorio del Calamita (Isola d'Elba). Atti del Convegno in memoria di Lamberto Pannuzi, Rossano 19-21 maggio 2005. Mem. Descr. Carta Geologica d'Italia, 78, 113-126.

D'Orefice M., Graciotti R. (2015) - Rilevamento geomorfologico e cartografia: realizzazione, lettura, interpretazione. Dario Flaccovio Editore s.r.l., pp. 360, Palermo.

D'Orefice M., Graciotti R. (Eds.) (2018) - Note illustrative della Carta Geomorfologica d'Italia alla scala 1.50.000, Fogli 316-317-328-329 "Isola d'Elba". Serv. Geol. d'It. - ISPRA, pp. 224.

D'Orefice M., Graciotti R., Capitanio F. (2007) - Le eoliani-ti dell'Isola d'Elba: i depositi del promontorio del M. Calamita e del Golfo di Viticcio. Il Quaternario, 20 (1), 21-44.

D'Orefice M., Foresi M.L., Graciotti R. (2011) - First recovery of marine quaternary deposits from geognostic boreholes of the coastal plain of Marina di Campo (Elba island): preliminary results. Il Quaternario, 26 (Abstract AIQUA, Roma, 02/2011), 29-31.

Douka K., Higham T. F. G., Hedges R. E. M. (2010) - Radiocarbon dating of shell carbonates: old problems and new solutions. MUNIBE Suplemento - Gehigarria 31, 18-27.

Fedi M., Cartocci A., Manetti M., Taccetti F., Mandò P.A. (2007) - The ^{14}C AMS facility at LABEC, Florence, Nucl. Instr. Meth. B 259, 18-22.

Ferranti L., Antonioli F., Amorosi A., Dai Prà G., Mastronuzzi G., Mauz B., Monaco C., Orrù P., Pappalardo M., Radtke U., Renda P., Romano P., Sansò P., Verrubbi V. (2006) - Elevation of the last interglacial highstand in Italy: A benchmark of coastal tectonics. Quaternary International, 145,146, 30-54.

Ferranti L., Antonioli F., Anzidei M., Monaco C., Stocchi P. (2010) - The timescale and spatial extent of vertical tectonic motions in Italy: insights from relative sea-level changes studies. Journal of the Virtual Explorer, Electronic Edition, ISSN 1441-8142, 36, paper 30.

Forzoni A., Storms J. E. A., Reimann T., Moreau J., Jouet, G. (2015) - Non-linear response of the Golo River system, Corsica, France, to Late Quaternary climatic and sea level variations. Quaternary Science Reviews, 121, 11-27.

Ghilardi M., Vacchi M., Currás A., Müller Celka S., Theurillat T., Lemos I., Pavlopoulos K. (2018) - Géoarchéologie des paysages littoraux le long du golfe sud-eubéen (île d'Eubée, Grèce) au cours de l'Holocène. Quaternaire, 29(2), 95-120.

Gischler E., Gibson M. A., Oschmann W. (2008) - Giant Holocene Freshwater Microbialites, Laguna Bacalar, Quintana Roo, Mexico. Sedimentology, 55, 1293-1309.

Graciotti R., Foresi L., Pantaloni M. (2004) - Lineamenti geomorfologici dell'Isola di Pianosa. Soc. Tosc. Scien. Nat. Atti serie A, 108, 95-111.

Green O.R. (2001) - Washing and Sieving Techniques Used in Micropalaeontology. In: A Manual of Practical Laboratory and Field Techniques in Palaeobiology. Springer, Dordrecht, 146-153

ISPRA-Servizio Geologico d'Italia (2015) - Carta Geologica d'Italia alla scala 1:50.000 - Fogli 316-317-328-329 "Isola d'Elba". http://www.isprambiente.gov.it/Media/carg/328_ISOLA_DELBA/Foglio.html

ISPRA-Servizio Geologico d'Italia (2018) - Carta Geomorfologica d'Italia alla scala 1:50.000. Foglio 316-317-328-329 "Isola d'Elba". ISPRA-Servizio Geologico d'Italia.

Jalut G., Dedoubat J.J., Fontugne M., Otto T. (2009) - Holocene circum-Mediterranean vegetation changes: Climate forcing and human impact. Quaternary International, 200, 4-18.

Lambeck K., Purcel A. (2004) - Sea-level change in the Mediterranean Sea since the LGM: model predictions for tectonically stable areas. Quaternary Science Reviews, 24, 1969-1988.

Lambeck K., Yokoyama Y., Purcell T. (2002) - Into and out of the Last Glacial Maximum: sea-level change during Oxygen Isotope Stages 3 and 2. Quaternary Science Reviews, 21, 343-360.

Lambeck, K., Antonioli, F., Anzidei, M., Ferranti, L., Leoni, G. (2011) - Sea level change along Italian coast during Holocene and a projection for the future. Quaternary International, 232 (1-2), 250-257.

Lambeck K., Rouby H., Purcel A., Yiying S., Sambridge M. (2014) - Sea-level and global ice volumes from Last Glacial Maximum to the Holocene. PNAS, 111(43), 15296-15303.

Maineri C., Benvenuti M., Costagliola P., Dini A., Lattanti P., Ruggieri G., Villa I. M. (2003) - Sericitic alteration at the La Crocetta deposits (Elba Island, Italy): interplay between magmatism, tectonic and hydrotermal activity. Mineralium Deposita, 38, 67-86.

Mayewski P.A., Rohling E.E., Stager J.C., Karlen W., Maasch K.A., Meeker L.D., Meyerson E.A., Gasse F., Van Kreveld S., Holmgren K., Lee-Thorp J., Rosqvist G., Rack F., Staubwasser M., Schneider R.R., Steig E.J. (2004) - Holocene climate variability. Quaternary Research, 62, 243-255.

Melis R.T., Depalmas A., Di Rita F., Montisa F., Vacchi M. (2017) - Mid to late Holocene environmental changes along the coast of western Sardinia (Mediterranean Sea). Glob. Planet. Chang., 155, 29-41.

Melis R. T., Di Rita F., French C., Marriner N., Montis F., Serreli G., Sulas F., Vacchi M. (2018) - 8000 years of coastal changes on a western Mediterranean island: A multiproxy approach from the Posada plain of Sardinia. Marine Geology, 403, 93-108.

Milli S., Mancini M., Moscatelli M., Stigliano F., Marini M., Cavinato G.P. (2016) - From river to shelf, anatomy of a high-frequency depositional sequence: The Late Pleistocene to Holocene Tiber depositional sequence. Sedimentology, 63, 1886-1928.

Pascucci V., De Falco G., Del Vais C., Sanna I., Melis R.T., Andreucci S. (2018) - Climate changes and human impact on the Mistras coastal barrier system (W Sardinia, Italy). Mar. Geol., 395, 271-284.

Peltier, W.R., Fairbanks, R.G. (2006) - Global glacial ice volume and last glacial maximum duration from an extended Barbados sea level record. Quaternary Science Reviews, 25, 3322-3337.

Posamentier H.W., Allen G.P. (1999) - Siliciclastic Sequence Stratigraphy - Concepts and Applications. Soc. Econ. Paleontol. Miner., Concepts in Sedimentology and Paleontology, 7, pp. 204.

Posamentier H.W., Jervey M.T., Vail P.R. (1988) - Eustatic controls on clastic deposition I: Conceptual framework. In: Sea Level Changes: An Integrated Approach (Ed. by Wilgus C.K., Hastings B.S., Kendall C.G.St.C., Posamentier H.W., Ross C.A., Van Wagoner J.C.). SEPM Special Publication, 42, 109-124.

Principi G., Bortolotti V., Pandeli E., Fanucci F., Moretti S., Innocenti F., D'Orefice M., Graciotti R. (2015a) - Carta geologica dell'Isola d'Elba scala 1:25.000. DREAm. Italia.

Principi G., Fanucci F., Bortolotti V., Chiari M., Dini A., Fazzuoli M., Menna F., Moretti S., Nirta G., Pandeli E., Reale V. (2015b) - Note Illustrative della Carta Geologica d'Italia alla scala 1:50.000 - Fogli 316-317-328-329 "Isola d'Elba". ISPRA-Dipartimento Difesa del Suolo-Servizio geologico d'Italia. http://www.isprambiente.gov.it/Media/carg/note_illustrative/328_Isola_DElba.pdf

Reimer P.J., Bard E., Bayliss A., Beck J. W., Blackwell P.G., Bronk Ramsey C., Grootes P.M., Guilderson T.P., Haflidason H., Hajdas I., Hatté C., Heaton T.J., Hoffmann D.L., Hogg A.G., Hughen K.A., Kaiser K.F., Kromer B., Manning S.W., Niu M., Reimer R.W., Richards D.A., Scott E.M., Southon J.R., Staff R.A., Turney C.S. M., van der Plicht J. (2013) - IntCal13 and Marine13 Radiocarbon Age Calibration Curves 0-50,000 Years cal BP. Radiocarbon, 55(4), 1869-1887.

Roberts N., Brayshaw D., Kuzucuoğlu C., Perez R., Sadori L. (2011) - The mid-Holocene climatic transition in the Mediterranean: Causes and consequences. The Holocene, 21(1), 3-13.

Sadori L. (2018) - The Lateglacial and Holocene vegetation and climate history of Lago di Mezzano (central Italy). Quaternary Science Reviews, 202, 30-44.

Saupé P., Marignac C., Moine B., Sonet J., Zimmerman J.L. (1982) - Datation par les méthodes K/Ar et Rb/Sr de quelques roches de la partie orientale de l'ile d'Elbe (Province de Livourne, Italie). Bull. Mineral., 105, 236-245.

Siddall M., Rohling E.J., Almogi-Labin A., Hemleben C., Meischner D., Schmelzer I. (2003) - Sea level fluctuations during the Last Glacial Cycle. Nature, 423, 853-858.

Suter J. R., Berryhill H.L. (1985) - Late Quaternary shelf-margin deltas, Northwest Gulf of Mexico. AAPG Bulletin, 69(1), 77-91.

Vacchi, M., Marriner, N., Morhange, C., Spada, G., Fontana, A., Rovere, A. (2016) - Multiproxy assessment of Holocene relative sea-level changes in the western Mediterranean: sea-level variability and improvements in the definition of the isostatic signal. Earth Sci. Rev., 155, 172-197.

Vacchi M., Ghilardi M., Spada G., Currás A., Robresco S. (2017) - New insights into the sea-level evolution in Corsica (NW Mediterranean) since the late Neolithic. J. Archaeol. Sci., Report 12, 782-793.

Vacchi M., Ghilardi M., Melis R.T., Spada G., Giaime M., Marriner N., Lorscheid T., Morhange C., Burjachs F., Rovere A. (2018) - New relative sea-level insights into the isostatic history of the Western Mediterranean. Quaternary Science Review, 201, 396-408.

Vigliotti L., Roveri M., Capotondi L. (2003) - Etruscan archaeo-metallurgy record in sediments from the Northern Tyrrhenian Sea. Journal of Archaeological Science, 30, 809-815.

Zaitlin B.A., Dalrymple R. W., Boyd R. (1994) - The stratigraphic organization of incised-valley systems associated with relative sea-level change. In: Incised-Valley Systems: Origin and Sedimentary Sequences (Ed. by Dalrymple R.W., Boyd R. & Zaitlin B.A.). Soc. Econ. Paleontol. Mineral., Spec. Publ., 51, 45-60.

Zecchini M. (1981) - L'Isola d'Elba dal Paleolitico all'epoca romana. In: "Studi sul territorio livornese: Archeologia, antropologia, geologia" a cura del Centro Livornese di studi archeologici. Editrice

La Fortezza, Livorno, 155-191.
Waelbroeck C., Labeyrie L., Michel E., Duplessy J.-C., McManus J., Lambeck K., Balbon E., Labracherie M. (2002) - Sea-level and deep water temperature changes derived from benthic foraminifera isotopic records. Quaternary Science Review 21, 295-305.

Ms. received: March 21, 2019 *Revised: January 21, 2020,*
Accepted: January 22, 2020 *Available online: January 29, 2020*